PHYSICAL REVIEW A VOLUME 30, NUMBER 1 JULY 1984

Measurements of L-Auger spectra of Pu, Am, Cf, and Fm and comparison with theory

S. K. Haynes
Department of Physics, Michigan State University, East Lansing, Michigan 48824

Melvin S. Freedman and Fred T. Porter*
Chemistry Division, Argonne National Laboratory, Argonne, Illinois 60439
(Received 27 December 1983)

The L-Auger spectra of $^{239}_{94}$Pu (64 lines), $^{254}_{100}$Fm (54 lines), $^{241}_{95}$Am (41 LMM lines only), and $^{250}_{98}$Cf (35 LMM lines only) were scanned over the range 6—19 keV at high resolution $(10^{-3} \leq \Delta E/E \leq 2\times 10^{-3})$ in the Argonne National Laboratory iron-free double toroidal spectrometer using thin ($\leq 1\ \mu$g/cm^2) isotopically separated radioactive sources. The observed energies of lines or line complexes agreed with Larkins's semiempirical predictions within the combined (theoretical plus experimental) standard deviations (1 s.d. = 10—20 eV in 10—20 keV) in 78% of the comparisons, and 19% were within 1—2 s.d. The measured intensities (relative to $L_3M_4M_5$) for Pu were compared to nonrelativistic predictions of McGuire for $Z=90$, with the relativistic predictions of Chen *et al.* for $Z=94$, and with a mixed system using Chen *et al.* for Coster-Kronig and McGuire for L-Auger transitions. Fm intensities (and Am and Cf qualitatively) could be compared only to relativistic theories. Relativistic predictions are clearly better for Pu, but are not, in general, satisfactory for either Pu or Fm; for all Pu and Fm lines, taken together, 58% are within 1 s.d., 30% in the range 1—2 s.d., and 12% greater than 2 s.d., with the relativistic predictions generally low except for the L_3MM band, which is in acceptable agreement. The ratio of the intense lines $I_{L_2M_4M_5}/I_{L_3M_4M_5}$ averaged for all four spectra is (27±7)% above the relativistic prediction. The first clearly resolved spectator vacancy satellites of Auger lines were seen in ^{241}Am and ^{250}Cf, and Coster-Kronig coefficients were deduced from their intensities relative to the main line. Their displacements in ^{241}Am agree with calculations of Shirley. Intermediate coupling components of some Auger lines were also first resolved and their relative intensities observed to fit the nonrelativistic calculations of Haynes. From the relative intensities of the M- and N-shell internal conversion lines of the 18.249-keV transition in ^{239}Pu, an $M1$ multipolarity is assigned.

I. INTRODUCTION

During radioactive decay studies[1-4] at Argonne National Laboratory of the complex internal conversion electron spectra of $^{239}_{94}$Pu, $^{241}_{95}$Am, $^{250}_{98}$Cf, and $^{254}_{100}$Fm, the L-Auger electron line spectra in the 6—19-keV range were also scanned. The sweeps were made at high resolution $(0.1\% \leq \Delta E/E \leq 0.2\%)$ with the Argonne double toroidal iron-free β spectrometers using very thin ($\sim 1\ \mu$g/ cm^2) isotopically separated sources. Thus we observed line shapes suffering minimal instrumental distortion in which intrinsic properties of the transitions such as natural widths (Sec. IV), intermediate coupling multiplet splittings (Sec. VII), spectator vacancy satellites (Sec. IV), and Doppler-shift—generated characteristic line-shape distortions (Sec. VI) could be resolved and identified, and easily distinguished from much narrower internal-conversion lines (Sec. IV). Because no L-Auger spectra had been studied for transuranic elements and because relativistic effects should be more pronounced for these elements than for those of lower atomic number, a fairly complete L-Auger spectrum was run for each element.

At the time of the experiments no satisfactory theory existed for the energies of the various Auger lines. There had been, however, a nonrelativistic j-j coupling theory for transition probability developed by McGuire[5] as well as an L-S coupling, more relativistic theory for transition probabilities produced by Ibari, Asaad, and McGuire.[6] Subsequent to the experiments, Larkins[7] developed a semiempirical theory for Auger energies (i.e., using empirical electron binding energies) and Chen *et al.*[8,9] computed transition probabilities on a relativistic j-j coupling basis. Therefore these spectra offer for the first time an opportunity to test the adequacy of these theories in the most relativistic and most "j-j" part of the Periodic Table.

II. EXPERIMENTAL PROCEDURES

Sources for these studies were prepared by chemical separation of reactor or cyclotron irradiated targets using ion exchange. The electron spectrometer sources were deposited on 10—25-μg/cm^2 carbon films in the target position in the Argonne electromagnetic isotope separator as circular 1—3 mm diameter spots of order 1 monolayer, ($<1\ \mu$g/cm^2) thickness. To reduce penetration into the support film to, at most, one atom layer, the 50-keV ion beam was decelerated to 100 eV before impact. The source deposits quickly oxidized. Source intensities were of order 0.1 μCi.

The electron spectra were surveyed in the Argonne double toroidal iron-free magnetic β spectrometer.[10] In tandem configuration the instrumental resolution in momentum $(\Delta p/p)$ in these experiments varied from 0.05 to

0.11% full width at half maximum (FWHM) for source diameters of 1 to 3 mm, respectively, corresponding approximately to $0.1\% < \Delta E/E \leq 0.2\%$ in energy in the regime of interest here below 20 keV. The corresponding spectrometer transmissions are (4—10)% of 4π sr, respectively.

The spectrometer detector was a bare cleaved 1-mm-thick NaI(T1) scintillating crystal in the spectrometer vacuum coupled directly to the cathode of an RCA 8575 photomultiplier. Its detection efficiency for low-energy electrons has been carefully measured.[11] Spectra were automatically scanned and recorded. The individual papers[1–4] should be consulted for particular details.

A considerable yield of information was derived from these spectra: the very complex nuclear level schemes and nuclear transition probabilities and multipolarities,[1–4] complete K-Auger spectra;[2,3] precise (few eV) atomic electron binding energies for most inner orbitals out to near valence levels,[12] a proof of the linearity of Maxwellian electrodynamics,[13] a proof of the invariance and adiabaticity of core electron binding energies in heavy elements,[14] and now, finally, the L-Auger sea of data, including clear demonstrations of "spectator vacancy" satellites, resolved intermediate coupling L-Auger multiplets, and L-Auger transition widths.

III. RESULTING SPECTRA

Figures 1 and 2 show the Pu and Fm L-Auger spectra. Extraneous background has been subtracted and the data have been corrected for the energy-dependent efficiency of the spectrometer detector counter and decay corrected to zero time. The decay correction factors were typically large and widely varying, as these spectra were run late on these short-lived sources. Thus the large statistical fluctuations of the weakened activities govern the displayed apparent high rates at zero time. This is particularly obvious at the low end of the Cf spectrum, Fig. 3.

The Pu and Fm spectra were the best of the four, both from the standpoint of statistics and also because the percentage of primary L_1 vacancies (i.e., before Coster-Kronig transitions have altered the L_1:L_2:L_3 distribution) was the smallest. Low L_1 initial population results in smaller L_2 and L_3 spectator vacancy satellites and more reliable line shapes for stripping the spectra. The figure captions explain fully the system of line designation used in these figures.

IV. WIDTHS, SATELLITES, AND VACANCIES

We describe some features of spectral lines that one encounters in the identification procedure and stripping analysis. The most obvious distinction is the contrast of the very narrow widths of internal conversion lines (e.g., line C, Fig. 2, the L_2 line of the 39.881-keV transition in Fm at 13 230 eV) and the widths of well-resolved intense L-Auger lines (e.g., line 19, L_2-M_2M_2 at 12 966 eV). In the Fm spectrum the instrumental width (FWHM) in this region is $\sim$13 eV. The excess width contribution of the L_2 level[15] in Fm, $\sim$13 eV, folded with the instrumental width corresponds to the measured width of the internal conversion line C. The contributions of the extra width of the M_2 orbital,[15] $\sim$15 eV, taken twice, further increase the L-Auger (line 19) width to $\sim$28 eV. Such contrast is seen more dramatically in Fig. 4(a), where one sees the sharp little M_3 internal conversion line of the 15.2-keV transition in ^{241}Am [$\Delta p/p = 0.07\%$, $(\Delta p/p)_{\text{instrum}} = 0.05\%$] riding on the left shoulder of the satellite of the L_3-M_5M_5 Auger line at 10.5 keV. The L_3-M_5M_5 main line (unfolded component on right) is about threefold wider, and the satellite (left component) is much wider still, due to many unresolved components. The pure L_1-M_4M_5 line (no satellite) width is $\Delta p/p = 0.14\%$, twice that of the lower-energy M_3 internal conversion line. A counterexample is the huge width of the K-132.4 keV conversion line in ^{241}Am at 7 keV, Fig. 5, where the K-level width[15] of 109 eV dominates the instrumental width of $\simeq$5 eV.

Figure 4 shows selected examples of the more intense L-Auger lines with different relative intensities of spectator vacancy (SV) satellites (the broad lower-energy bulges on L_3- and L_2-Auger lines) in (a) Am, (b) Cf, and (c) Fm L-Auger transitions. The first evidence of spectator-vacancy-satellite broadening and shifting on L-Auger lines was seen in ^{210}Bi by Haynes *et al.*[16] Here in Am especially we see the first clean resolution of the satellite complex from the main Auger line.[17] Such satellites of L_3 Augers (to a lesser extent of L_2) are associated with that fraction of L_3 (or L_2) vacancies which are created by Coster-Kronig (CK) transitions from L_1 and L_2 vacancies. Such CK transitions produce vacancies in M,N shells whose lifetimes are comparable to or longer than the resulting L_3 (or L_2) vacancies. Thus the subsequent L_3- (or L_2-) Auger transitions are shifted, usually downward, in energy with respect to the normal L_3- or L_2-Auger line, owing to the increases in binding energies of the remaining $M,N\ldots$ orbitals involved in the Auger transition because of the reduced screening of nuclear charge due to the spectator outer-orbital vacancy. Since there is a spectrum of such CK-induced outer vacancies, the result is a multitude of shifts in binding energies and an unresolved broad complex of satellite Auger lines.

An energy shift of -56 eV, Fig. 4(a), is observed between the main L_3-M_4M_5 Auger line (arising from primary L_3 vacancies in internal conversion) and the centroid of the broad satellite in Am. This shift compares favorably to the shift of -61 eV calculated by Shirley.[18]

The shape and splitting of the SV-main line complex is distinguishable from that of imperfectly resolved intermediate coupling (IC) multiplets (Sec. VII). For example, the splitting of the main IC components of L_3-M_4M_5 in Am is only $\sim$20 eV [nonrelativistically for Fm (cf. Sec. VII) and undoubtedly also for Am] and the lowest energy IC components $^3P_1$ plus $^1G_4$ have approximately five times the intensity of the highest $^1D_2$ component, compared to the observed SV splitting of 56 eV and the (SV to main line) intensity ratio of 1.5. Presumably, each (unresolved) IC component of an L_2 or L_3 line will have an associated SV satellite complex.

On the reasonable assumption that relative Auger transition probabilities within an L_i-MM band should be only little affected by the presence of spectator $M,N,\ldots$ vacancies, the ratio of SV satellite to main line intensity should be approximately constant within the L_i band, as is ob-

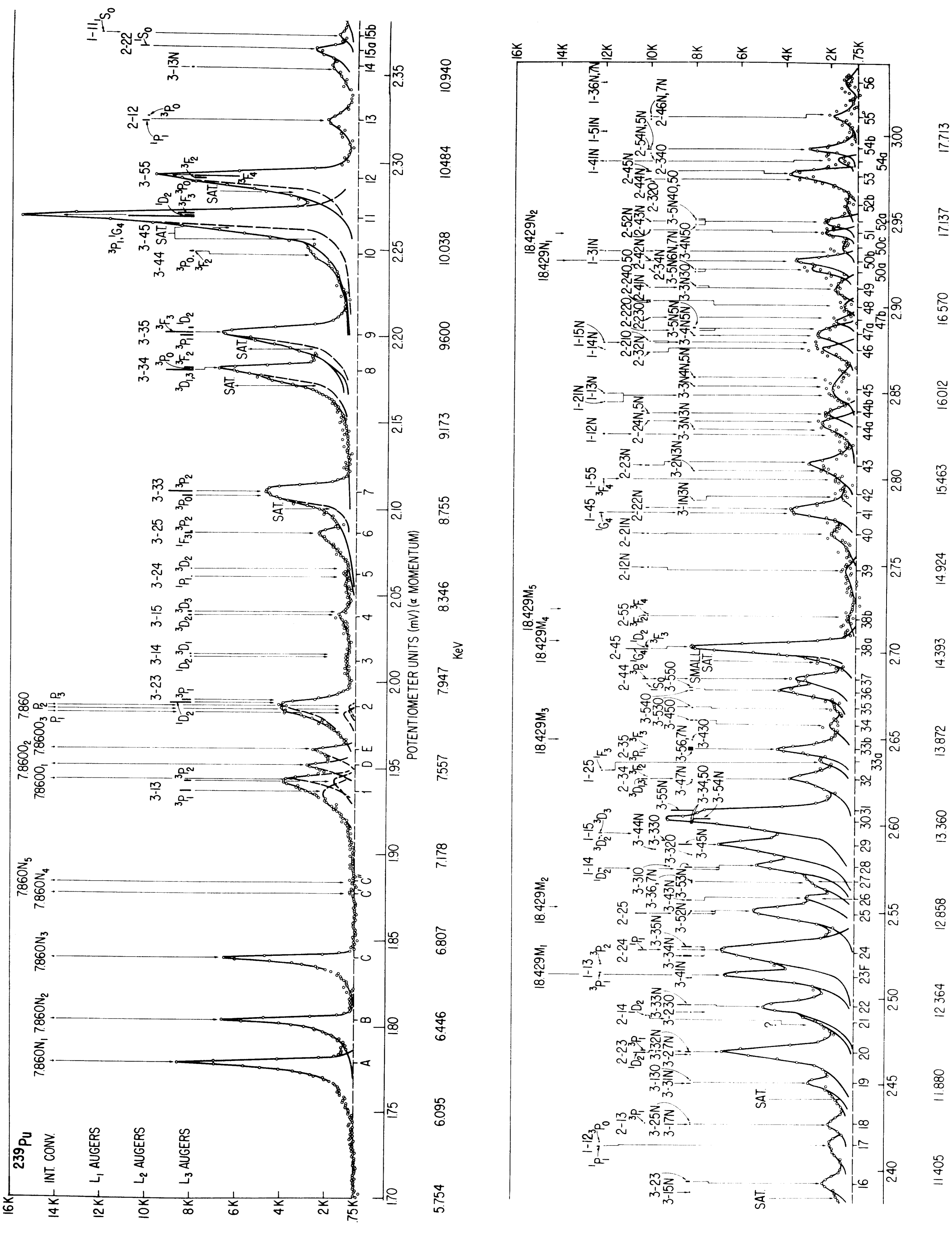

FIG. 1. L-shell Auger and internal conversion lines in ^{239}Pu. Labels i-jk denote L_i-M_jM_k Auger lines; i-$jPkQ$ denote L_i-P_jQ_k Auger lines. Heavy vertical bars show theoretical positions and relative intensities of intermediate coupling components of Auger lines. SAT denotes the location of reduced energy "spectator vacancy" satellite peaks of strong L_3 and L_2 Auger lines; see text Sec. IV.

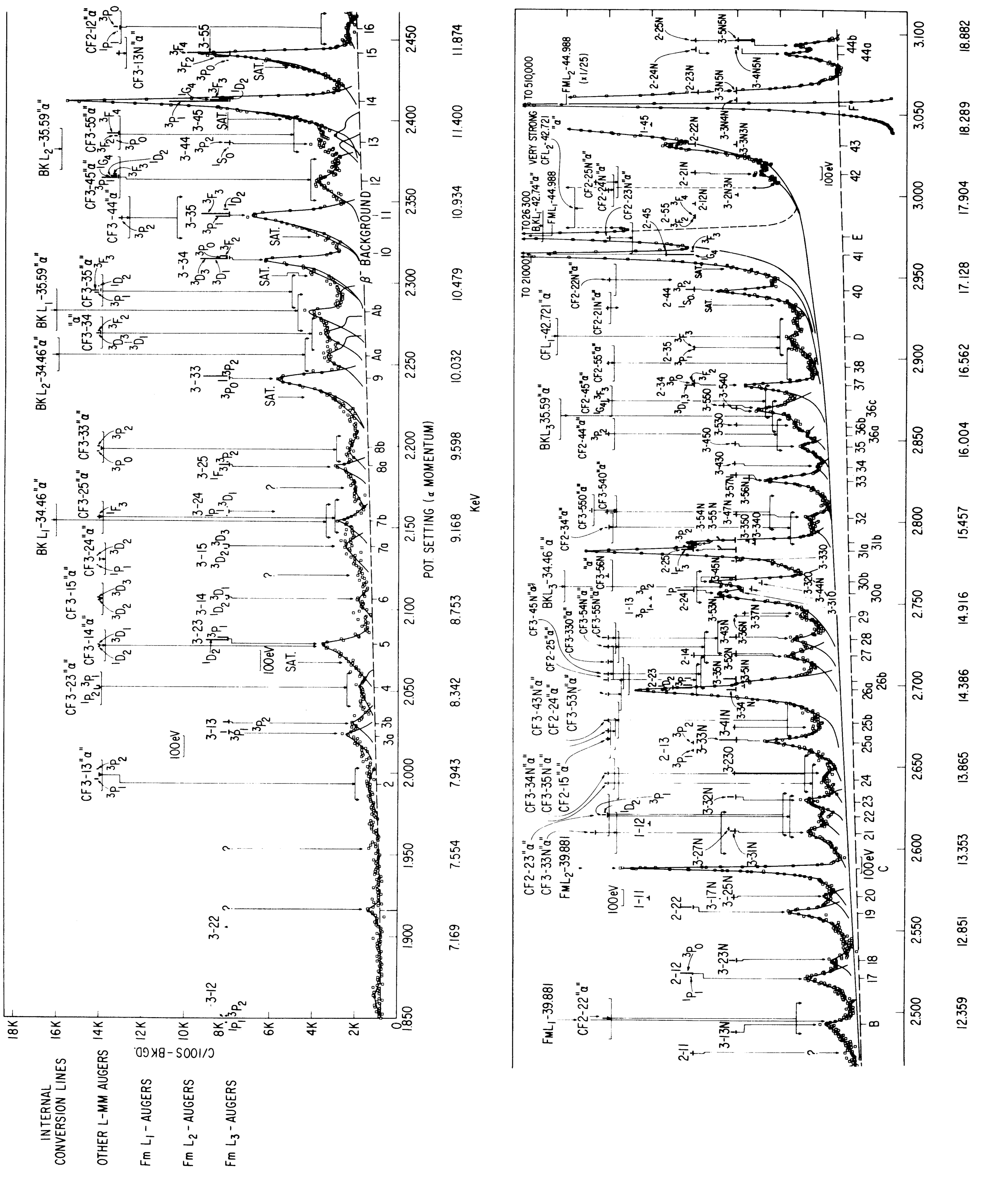

INTERNAL CONVERSION LINES
OTHER L-MM AUGERS
Fm L_1 - AUGERS
Fm L_2 - AUGERS
Fm L_3 - AUGERS
C/100S - BKGD.
POT. SETTING (α MOMENTUM)
KeV
β⁻ BACKGROUND
VERY STRONG
TO 510,000
TO 26,300
TO 21000

FIG. 2. L-shell Auger lines and internal conversion lines in ^{254}Fm, ^{250}Cf, and ^{250}Bk. Labels i-jk denote L_i-M_jM_k Auger lines; labels i-$jPkQ$ denote L_i-P_jQ_k Auger lines; labels left of intensity axis show approximate height of the line labels on Fm L_i-subshell Augers, on Cf Augers, and on internal conversion lines. Heavy vertical bars show theoretical positions and relative intensities of intermediate coupling components of Auger lines; below these are short horizontal bars centered at weighted average position of components which show theoretical energy uncertainty arising from experimental uncertainty in orbital binding energies used in calculations. Internal conversion lines are from transitions following the decays: $^{254m}_{99}\mathrm{Es} \xrightarrow[(39.3h)]{\beta} {}^{254}\mathrm{Fm}$ (primary source); 44.988 and 39.881 keV: $^{254}_{100}\mathrm{Fm} \xrightarrow[(3.2h)]{\alpha} {}^{250}_{98}\mathrm{Cf}$; 42.721 keV: $^{254}_{99}\mathrm{Es} \xrightarrow[(276d)]{\alpha} {}^{250}_{97}\mathrm{Bk}$; 42.74, 35.59, and 34.46 keV. The L Auger lines of Cf and the internal conversion lines of Cf and Bk are labeled α to denote the Doppler shift broadening; see text, Sec. VI; the broadening is shown by the horizontal bracket. SAT denotes the location of reduced energy "spectator vacancy" satellite peaks of strong L_3 Fm Auger lines; see text, Sec. IV.

TABLE I. Ratio of SV satellite to main L-Auger line intensities.

Isotope	Auger transitions	Ratio	Average	Theory[a]
^{254}Fm	$L_3M_4M_5$	0.22 ± 0.04		
			0.24 ± 0.04	0.22
	$L_3M_5M_5$	0.30 ± 0.15		
^{250}Cf	$L_3M_4M_5$	0.68 ± 0.15		
			0.84 ± 0.12	0.835
	$L_3M_5M_5$	1.0 ± 0.2		
^{241}Am	$L_3M_4M_5$	1.50 ± 0.15		
			1.67 ± 0.12	1.67
	$L_3M_5M_5$	1.85 ± 0.18		
	$L_2M_4M_4$	0.29 ± 0.05		
			0.23 ± 0.05	0.11
	$L_2M_4M_5$	0.18 ± 0.04		
	$L_1M_4M_5$	0		

[a]Reference 19(a).

served here (Table I), but see later discussion.

However, the ratio of satellite to main L-Auger line intensity for a given element should be largest for L_3 and less for L_2 due to the larger CK production of L_3 vacancies than L_2 vacancies, i.e., the CK coefficients $f_{13}+f_{23}>f_{12}$ for heavy elements; of course there can be no SV satellites for L_1-Auger lines. The L_3, L_2, and L_1 Augers plus satellites of Fig. 4(a) are consistent with those expectations and so the pure L_1 line can serve as a model in unfolding the main L_2 and L_3 lines from the satellites in Am and Cf. Indeed, the relative SV-satellite to main line-intensity ratio for L_3 and L_2 Augers (Table I) can yield, together with values for the primary L_1:L_2:L_3 vacancy ratios (Table II) independent values for the CK f_{ij} coefficients (Table III). The f_{13} and f_{23} coefficients are seen to be in fair agreement with the calculations of Chen *et al.*,[19(a)] the data evaluation of Krause,[19(b)] and the measured values for Cf,[20] but the (SV satellite to $L_2M_4M_{4,5}$) intensity ratios in ^{241}Am are much too large to be consistent with the evaluated or theoretical f_{12} values. This is quite unaccountable, especially in view of the fact that L_1-L_2 CK transitions in Am only become energetically possible at the N_5 subshell and SV's in $N_{6,7}$ and higher shells should generate only small satellite shifts.

Table II gives the L_i primary vacancy distribution obtained from the summed intensity ratios of $I_{L_1}/I_{L_2}/I_{L_3}$ internal conversion lines observed in the full electron spectrum of each decay[1–4] plus the L_1, L_2, and L_3 infeeds from K Augers and K x rays (from K internal conversion

TABLE II. L-subshell vacancy population before Coster-Kronig transitions (%).

	L_1	L_2	L_3
^{254m}Es (β^-) ^{254}Fm	2.5	54.7	42.8
^{250}Es (e.c.) ^{250}Cf	34	34	32
^{241}Cm (e.c.) ^{241}Am	55	23	22
^{239}Am (e.c.) ^{239}Pu	23	35	42

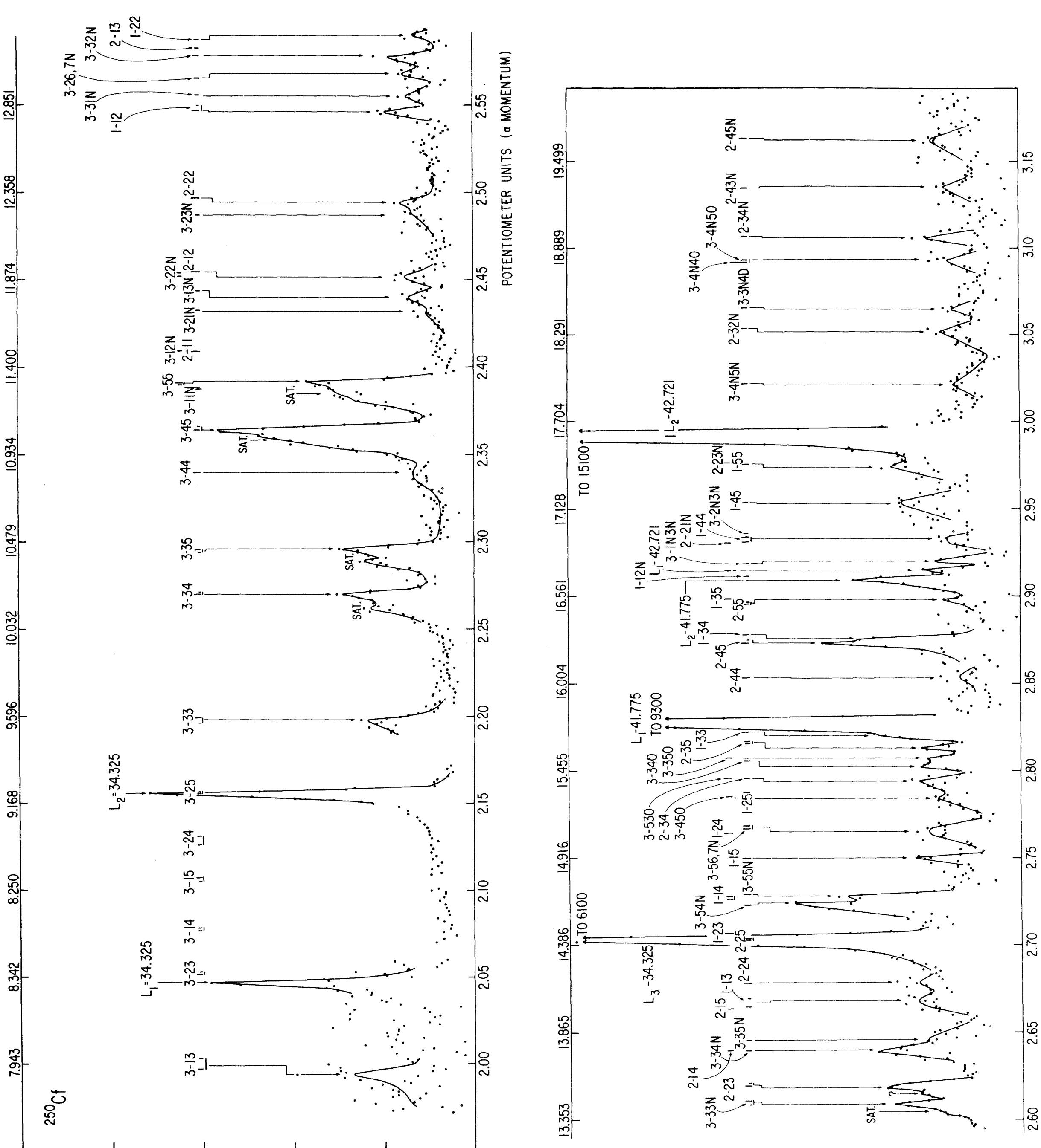

FIG. 3. *L*-shell Auger and internal conversion lines in ^{250}Cf; see caption of Fig. 1.

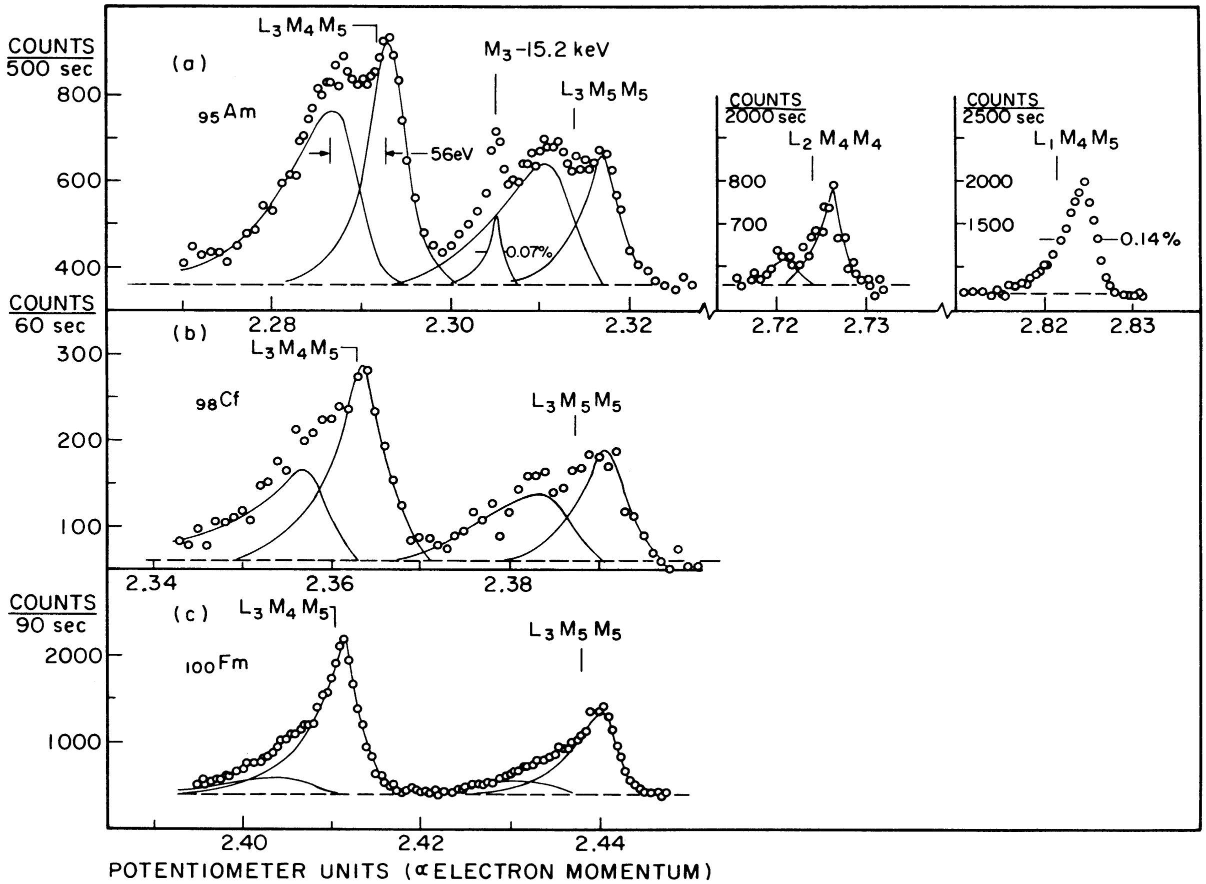

FIG. 4. Sample of strong L Auger lines from spectra of (a) ^{241}Am, (b) ^{250}Cf, and (c) ^{254}Fm showing (variation in) relative intensities of spectator vacancy satellites (lower energy, incompletely resolved components) of L_3 (and L_2) Auger peaks. L_1 Auger peaks, as expected, show no such satellites. Note the very narrow relative peak width of the M_3-15.2 keV conversion line near the L_3-M_5M_5 Auger line in ^{241}Am.

and K-electron capture), and from nuclear L_i-shell electron capture, as applicable. The relative intensities of SV satellite to main L_3-Auger lines are seen to vary from high, Am, to very low, Fm [Figs. 4(a)—4(c) and Table I] consistent with the variations in primary L_1 vacancy fractions, since L_1 is the principal CK source for L_3 vacancies in Am and Cf. There is weak evidence in the three L_3-M_4M_5 versus L_3-M_5M_5 (SV to main line) ratios in Table I that the presence of spectator vacancies may slightly influence relative Auger probabilities within a band.

V. IDENTIFICATION OF LINES

When an experimental Auger spectrum is to be compared with theory for energy and intensity the first problem is identification of peaks in these rich and complex spectra without using the theory to be tested. This requires some prior knowledge of energies and intensities. Fortunately, the L_3-MM spectra have some of the most intense lines and are generally free from interference by other lines. Also, comparison of several spectra of nearly the same atomic number is facilitated by the smooth regu-

TABLE III. Coster-Kronig coefficients

	This expt.[a]	$_{98}$Cf[b]	Theory[c]	Data[d] evaluation
f_{12}	0.096±0.02	0.068	0.045±0.003	0.04
f_{13}	0.60±0.05	0.594	0.62±0.02	0.54
f_{23}	0.16±0.03	0.123	0.20±0.02	0.198

[a]Average for $Z=95$—100, computed from Tables I and II, ignoring Z dependence.
[b]Reference 20.
[c]Reference 19(a); average of $Z=95,98,100$ values.
[d]Reference 19(b); average of $Z=95,98,100$ values.

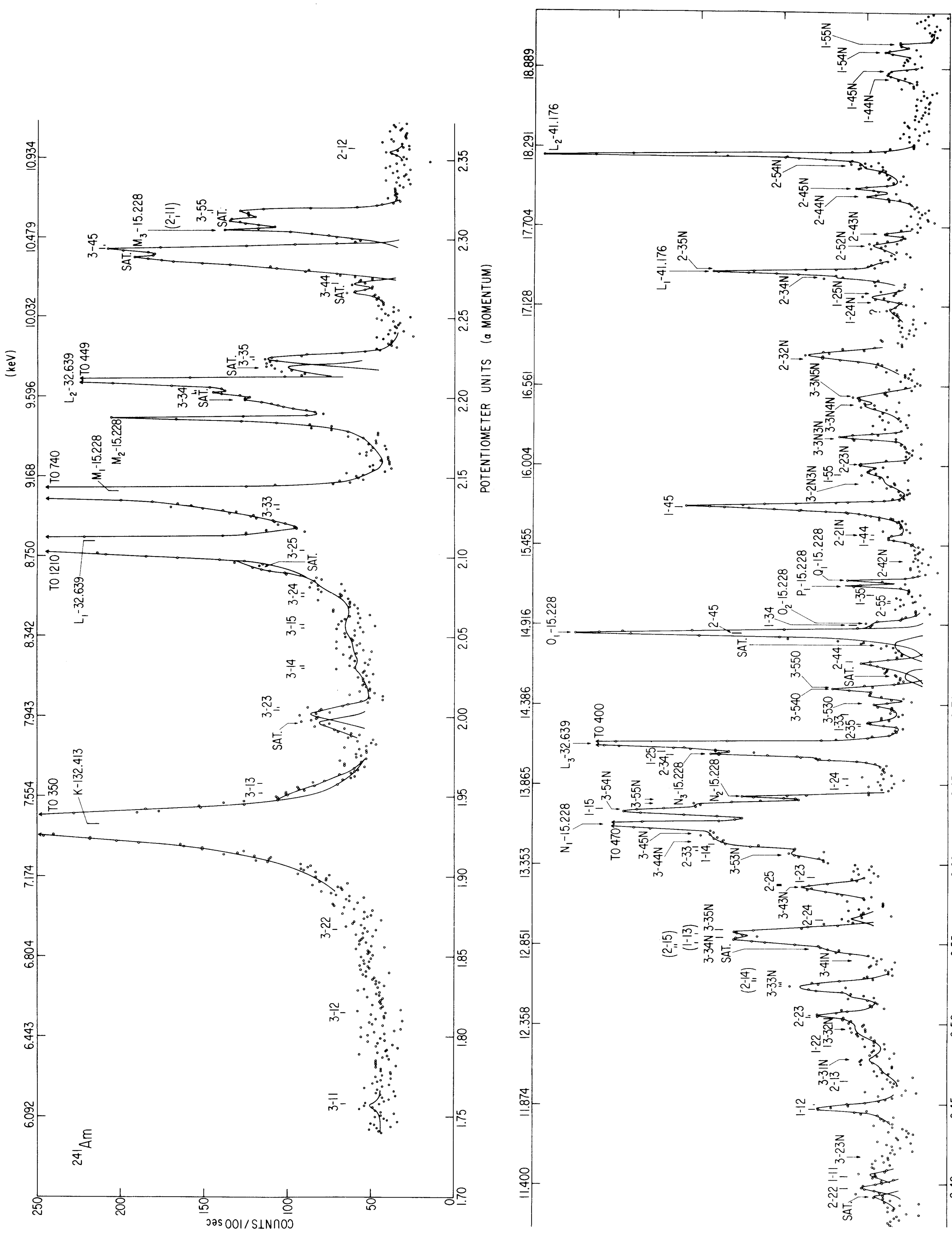

FIG. 5. L-shell Auger and internal conversion lines in ^{241}Am; see caption of Fig. 1.

lar Z-wise progression of electron binding and hence of L-Auger energies so that signature patterns of line group spacings come to be recognizable and transferable between spectra with only small Z-scaling adjustments. Resolution of a spectral region complicated by the accidental intrusion of intense internal conversion lines is greatly aided by comparison with the same but uncontaminated region of a nearby element. That each element's spectrum has widely different relative numbers of primary L_1, L_2, and L_3 vacancies enables one to sort out lines in the region where L_2-MM, L_1-MM, and L_3-MN overlap by Z-wise comparison. [${}^{210}_{82}\mathrm{Pb} \to {}^{210}_{83}\mathrm{Bi}$ is an outstanding example where the intense L_1 primary vacancies $V_{L_1}:V_{L_2}:V_{L_3} \approx 90:9:1$ (Ref. 16) lead to certain identifications of the usually inaccessible L_1-MM Auger structure.]

One starts with the $\Delta Z = 1$ (Ref. 21) approximation for line energies (i.e., $E=[B_{L_i}(Z)-B_{M_j}(Z)-B_{M_k}(Z+\Delta Z)]$, where the binding-energy terms are evaluated at Z or interpolated at $(Z+\Delta Z)$) and then, based on the above experiences, derives an expression for the approximate variation of ΔZ ($\Delta Z \leq 1$) across the band from L_i-M_1M_1 to L_i-M_5M_5.[16] By applying these rules for L-MM and L-NN, and $\Delta Z \sim 1$ for L-MN, L-MO, etc., identification becomes fairly positive and one can gradually develop some empirical rules identifying strong, medium, and weak lines where they are clearly resolved in some spectra, so that when lines cannot be resolved in another spectrum one has a good idea which is the most important. These empirical rules have been summarized by Haynes.[22]

The four elements studied here had primary L_1:L_2:L_3 vacancy ratios varying widely (Table II). For example, concerning the use made of these distributions in identifying lines, the low 3% initial L_1 vacancy population in Fm simplifies the spectrum in the region of line 30a (L_2-M_2M_4, L_3-M_5N_3), enabling their more confident identification and the transference of their pattern to the Pu spectrum with its intense $L_1M_1M_3$ line intruding (lines 23 and 24). Another example is the use of the different relative intensities of spectator vacancy satellites to characterize L_3, L_2, and L_1 Augers in Am [Fig. 4(a)].

By using the empirical rules for energy and intensity discussed above together with the comparison of the four spectra, unequivocal identification of the important lines becomes possible. Comparison of the four spectra, e.g., between potentiometer settings (proportional to electron momentum) 2.23 and 2.65 where the L_1-, L_2-, L_3-Auger energy overlap is the worst, shows that one can easily follow most transitions from one spectrum to another. Finally, with transitions located in energy and intensity, it becomes possible to make detailed comparisons with theory for energy and intensity without having used these theories for the identification of experimental lines.

VI. DETERMINATION OF EXPERIMENTAL ENERGIES AND INTENSITIES

Stripping Auger spectra is not an easy task. The basic instrumental line shape is constant throughout the spectrum with a width proportional to momentum. However, the single natural-level width of internal conversion lines and the various three-level width broadenings of L-Auger lines add measurably to the instrumental width and complicate this simple dependence. Moreover, the sources are not infinitely thin for these energies, leading to some energy degradations from deep atoms which results in further increases in line widths and especially in very long line tails which, increasingly at lower energy, distort still lower-lying lines.

Furthermore, most j-j designated lines are composed of several incompletely resolved components of different total angular momenta J which arise from the actually prevailing intermediate coupling. In addition, L_2 and L_3 lines have spectator vacancy satellites which themselves have more components than the main line and which are incompletely separated from the main line.

The Fm spectrum suffers further severe complications arising from the variety of nuclear decays in the source. The main sequential decays were

$$ {}^{254m}_{99}\mathrm{Es} \xrightarrow[\beta^-]{39\ \mathrm{h}} {}^{254}_{100}\mathrm{Fm} \xrightarrow[\alpha]{3.2\ \mathrm{h}} {}^{250}_{98}\mathrm{Cf}\ , $$

so that the 3 h α decay quickly grew to equilibrium in the source, yielding an intense Cf L-Auger spectrum owing to strong ^{250}Cf L-shell internal conversions. The spectrum thus contains complete Fm and Cf L Augers plus numerous Fm and Cf internal conversion lines in the range.

Both the Cf conversion and Auger lines strongly exhibit an extended high-energy shoulder with sharply defined upper cutoff and a broad low-energy tail (see Fig. 2, line 12). These features are more clearly visible on higher-energy lines above the dense L-Auger region. These distortions following α decay originate from electron emission from the moving recoil ions in the spectrometer vacuum within a few millimeters of the source spot (Doppler shifts) in that half of the Fm decays in which the α particle is emitted backwards into the source support foil. In the other half of the decays the recoil is stopped in the backing foil within 10^{-16} sec, much less than the lifetime of the $E2$ nuclear decays that produce internal conversion electrons and then L-Auger transitions; both of these produce the central-peak features without Doppler broadening, but with extended tailing from deep recoils.

Yet further complexity is due to the presence in the isotope-separator-deposited source of isobaric ${}^{254}_{99}$Es ground state which decays slowly:

$$ {}^{254}_{99}\mathrm{Es} \xrightarrow[\alpha]{276\ \mathrm{d}} {}^{250}_{97}\mathrm{Bk} \xrightarrow[\beta^-]{3\ \mathrm{h}} {}^{250}_{98}\mathrm{Cf}\ . $$

Thus one also sees weak internal conversion lines of ^{250}Bk with Doppler broadening, although the L-Auger lines of Bk are undetectably weak, and also, in principle, one sees a small enhancement of Cf lines.

We present detailed analyses of the two spectra, Pu and Fm, with the most reliable statistics and lowest intensity of spectator vacancy satellites (primary L_1 vacancies 23% and 2.5%, respectively). For Fm, strong conversion lines toward the upper end and middle of the spectrum give information on line tail shape and intensity as a function of energy. For Pu, conversion lines at the low-energy end of the spectrum show what the maximum tail effect is.

TABLE IV. *L*-Auger (and internal conversion) lines in ^{239}Pu. Asterisks (*) indicate those transitions which, according to the criteria of Haynes (Ref. 22) are expected to be the most important.

	Predicted Energy			Experimental[d]					Theoretical Intensity						Agreement[h]		
Pu Transition (Auger/ Conversion)	Energy (Spread) Larkins[a] (eV)	Unc.[b]	Intm. Coup. %[c]	Line[d]	Energy (eV)	Unc.	Int.	Unc.	Non-Rel.[e] Z=90	Line Groups	Mixed[f] NR,Z=90 R,Z=94	Line Groups	Rel.[g] Z=94	Line Groups	Energy	Int.	Qual. Evid.
L_3-M_1M_1	6095	3					0	0.005	0.006		0.006		0.004		-	R	VW
7860 N_1	6297	3		A	6297	2	0.470	0.02									
7860 N_2	6476	5		B	6473	2	0.330	0.02									
L_3-M_1M_2	6489-6514	6					0	0.005	0.008		0.008		0.002		-	R	VW
7860 N_3	6733	6		C	6732	2	0.316	0.01									
L_3-M_2M_2	6861	7					0	0.005	0.003		0.003		<<0.001		-	ALL	VW
7860 N_4	7010	3		C'	7014	7	0.010	0.005									
7860 N_5	7058	3		C"	7063	11	0.005	0.005									
L_3-M_1M_3 $^3P_1$	7452	6	61%	1	7439	10	0.19	0.05	0.108		0.108		0.205		E	R	M
$^3P_2$	7498	6	39%		7500	15											
7860 O_1	7506	6			7515	10	0.13	0.05									
7860 O_2	7573	6		D	7567	3	0.097	0.02									
7860 O_3	7643	4		E	7639	2	0.096	0.02									
7860 P_1	7810	6		2			0.06	0.05									
7860 $P_{2,3}$	7820-7840	4															
L_3-M_2M_3	7849-7861	7			7850	9	0.29	0.05	0.233		0.233		0.344		E	NONE R,B	M
L_3-M_1M_4	8057-8070	3		3	8050	24	0.011	0.005	0.018		0.018		0.034		G	NR,M	W
L_3-M_1M_5	8248-8265	3		4	8257	8	0.045	0.020	0.017		0.017		0.071		G	NONE R,B	W
L_3-M_2M_4	8428-8468	5		5	8426	20	0.02	0.02	0.022		0.022		0.015		G	ALL	VW
L_3-M_2M_5	8634-8642	5		6	8639	8	0.103	0.02	0.178		0.178		0.102		E	R	S
L_3-M_3M_3	8814-8839	7		7	8841	9	0.368	0.03	0.357		0.357		0.403		G	NR,M	S
L_3-M_3M_4	9423-9436	5		8	9435	5	0.376	0.03	0.350		0.350		0.416		F	NR,M	S
L_3-M_3M_5 $^3P_1$,$^3F_3$	9598-9611	5	90%	9	9612	5	0.547	0.04	0.586		0.586		0.524		E	ALL	S
$^1D_2$,$^3F_4$	9635-9650	5	10%														
L_3-M_4M_4	9991-10022	2		10	10005	14	0.038	0.02	0.052		0.052		0.053		G	ALL	W
L_3-M_4M_5 $^3P_1$$^1G_4$	10201-10202	2	72%	11	10207	4	1.000	-	1.000	1.003	1.000	1.002	1.000	1.002	G	STD.	VS
$^1D_2$$^3F_3$	10209-10222	2	28%														
L_2-M_1M_1	10304	3							0.003		0.002		0.002		-	ALL	VW
L_3-M_5M_5 $^3F_2$,$^3F_4$	10402-10413	2	95%	12	10417	5	0.714	0.04	0.699		0.699		0.666		G	NR,M	S
$^3P_0$	10375	2	5%														
L_3-M_1N_1	10511-10526	5					0	0.01	0.002		0.002		N		-	ALL	VW
L_3-M_1N_2	10700-10702	5					0	0.01	0.002		0.002		N				
L_2-M_1M_2 $^3P_0$	10723	6	16%	13	10703	6	0.094	0.02	0.049	0.051	0.032	0.034	0.095	0.095	G	R	S
$^1P_1$	10698		84%														
L_3-M_2N_1	10901-10903	7					0	0.01	0.002		0.002		N		-	ALL	VW
L_3-M_1N_3	10957-10961	6		14	10964	10	0.040	0.02	0.017		0.017		0.034		E	R	W
L_2-M_2M_2*	11070	7		15a	11066	9	0.107	0.02	0.061	0.062	0.040	0:041	0.103	0.103	E	R	S
L_3-M_2N_2	11073-11088	7							0.001		0.001		N				
L_1-M_1N_1	11142	6		15b	11146	19	0.02	001	0.009		0.008		0.023		E	ALL R,B	W
L_3-M_1N_4	11241-11242	3							0.003		0.003		0.004				
L_3-M_1N_5	11288-11289	3							0.003	0.045	0.003	0.045	0.008	0.069		R,B	M
L_3-M_2N_3*	11340-11341	7		16	11338	6	0.087	0.02	0.039		0.039		0.057		G	R	M
L_1-M_1M_2	11536-11561	7		17	11548	12	0.059	0.02	0.022		0.022		0.048		G	R	M
L_3-M_2N_4	11621-11624	5							0.005		0.005		0.003				
L_3-M_1N_6	11649-11651	3							0.004		0.004		<0.005				
L_3-M_1N_7	11661-11663	3		18	11659	9	0.055	0.02		0.049		0.047	0.007	0.039	G	ALL NR,M,B	M
L_3-M_2N_5*	11670-11671	5							0.033		0.033		0.016				
L_2-M_1M_3	11661-11707	6							0.007		0.005		0.008				
L_3-M_1O_1	11754	5							0.001		0.001		N				
L_3-M_1O_2	11824	6							N		N		N				
L_3-M_3N_1*	11883-11887	7		19	11891	9	0.078	0.02	0.029	0.034	0.029	0.034	0.055	0.062	E	R	M
L_3-M_1O_3	11905	3							0.004		0.004		0.007				

TABLE IV. (*Continued*).

	Predicted Energy			Experimental[d]					Theoretical Intensity						Agreement[h]		
Pu Transition (Auger/ Conversion)	Energy (Spread) Larkins[a] (eV)	Unc.[b]	Intm. Coup. %[c]	Line[d]	Energy (eV)	Unc.	Int.	Unc.	Non-Rel.[e] Z=90	Line Groups	Mixed[f] NR,Z=90 R,Z=94	Line Groups	Rel.[g] Z=94	Line Groups	Energy	Int.	Qual. Evid.
L_1-M_2M_2	11908	9							N		N		N				
L_3-M_1O_4	12008	6							0.001		0.001		N				
L_3-M_1O_5	12018	6							0.001		0.001		0.002				
L_3-M_2N_6	12029-12035	6							0.006		0.006		<0.004				
L_3-M_2N_7	12043-12044	6											0.008				
L_2-M_2M_3*	12058-12070	7		20	12063	6	0.341	0.035	0.214	0.278	0.141	0.205	0.219	0.311	E	R	S
L_3-M_3N_2*	12065-12066	7							0.056		0.056		0.082				
L_3-M_2O_1	12135	7							N		N		N				
L_3-M_2O_2	12205	7							N		N		N				
L_2-M_1M_4	12266-12279	3		21	12240	22	0.027	0.02	0.003	0.012	0.002	0.011	0.019	0.032	F	ALL R,B	VW
L_3-M_2O_3*	12286	7							0.009		0.009		0.013				
L_3-M_3N_3	12309-12331	7		22	12306	10	0.235	0.02	0.147		0.147		0.171		G	NONE R,B	S
L_3-M_2O_4	12389	7							N		N		N				
L_3-M_2O_5	12399	5							0.007		0.007		0.003				
L_2-M_1M_5	12457-12474	3							0.014		0.009		0.006				
L_3-M_4N_1	12481-12483	4							0.004		0.004		0.008				
18429 M_1	12496	8		23F	12501	5	0.210	0.02	~0.13	[0.210][i]	~0.14	[0.210][i]	~0.13	[0.210][i]	E	ASS.	S
L_1-M_1M_3*	12499-12545	7							0.051		0.045		0.064				
L_3-M_3N_4*	12603-12609	5							0.081		0.081		0.098				
$^1P_1$*	12637	5	98%														
L_2-M_2M_4				24	12636	10	0490	0.03	0.123	0.344	0.080	0.301	0.114	0.356	E	NONE NR,R,B	S
$^3P_2$	12677	5	2%														
L_3-M_3N_5*	12649-12656	5							0.132		0.132		0.123				
L_3-M_4N_2	11661-12664	4							0.005		0.005		0.004				
L_3-M_5N_1	12675-12678	4							0.003		0.003		0.017				
L_2-M_2M_5*	12843-12851	5							0.224		0.147		0.140				
L_3-M_5N_2*	12857-12858	4		25	12860	5	0.204	0.02	0.054	0.292	0.054	0.216	0.022	[0.204][i]	F	ASS.	S
18429 M_2	12882	9							0.017+		0.019+		0.042				
L_1-M_2M_3	12896-12908	9		26	12932	10	0.065	0.02	0.003	0.044	0.002	0.043	0.001	0.066	F	R	M
L_3-M_4N_3*	12918-12924	4							0.041		0.041		0.065				
L_2-M_3M_3	13023-13048	7							0.006		0.004		0.004				
L_3-M_3N_6*	13012-13019	6		27	13024	15	0.055	0.02	0.027	0.033	0.027	0.031	0.011	0.029	E	NR	W
L_3-M_3N_7*	13021-13030	6											0.014				
L_1-M_1M_4*	13104-13117	6							0.045		0.039		0.044				
L_3-M_5N_3*	13111-13118	5		28	13120	6	0.150	0.02	0.108	0.160	0.108	0.154	0.092	0.150	G	ALL	M
L_3-M_3O_1	13119	7							0.007		0.007		0.014				
L_3-M_3O_2*	13189	7							0.014		0.014		0.020				
L_3-M_4N_4	13187-13209	2							0.021		0.021		0.021				
L_3-M_4N_5*	13247-13254	2							0.161		0.161		0.162				
L_3-M_3O_3*	13270	7		29	13246	5	0.326	0.03	0.034	0.297	0.034	0.277	0.041	0.299	E	NONE NR,R	S
L_1-M_1M_5*	13295-13312	6							0.067		0.047		0.055				
L_3-M_3O_4*	13373	5							0.017		0.017		0.020				
L_3-M_3O_5*	13383	5							0.028		0.028		0.025				
L_3-M_5N_4*	13395-13401	2		30	13388	{+5, −10}	0.632	0.03	0.206	0.517	0.206	0.517	0.197	0.493	E	NONE NR,M,B	S VS
L_3-M_5N_5*	13437-13454	2		31	13449	10			0.265		0.265		0.247				
L_1-M_2M_4	13475-13515	7							0.001		0.001		0.004				
L_3-M_4N_6	13605-13620	3							0.032		0.032		0.006				
L_3-M_4N_7*	13622-13628	3		32	13632	6	0.154	0.02		0.204		0.145	0.020	0.109	E	M	S
L_2-M_3M_4*	13632-13645	7							0.172		0.113		0.083				
L_1-M_2M_5	13681-13689	7							0.020		0.017		0.021				
L_3-M_4O_1	13717	4		33a	13730	12	0.04	0.02	0.001	0.022	0.001	0.029	0.002	0.023	˙P	ALL M,B	W
L_3-M_4O_2	13787	5							0.001		0.001		N				

TABLE IV. (*Continued*).

Pu Transition (Auger/ Conversion)	Predicted Energy: Energy (Spread) Larkins[a] (eV)	Unc.[b]	Intm. Coup. %[c]	Experimental[d]: Line[d]	Energy (eV)	Unc.	Int.	Unc.	Theoretical Intensity: Non-Rel.[e] Z=90	Line Groups	Mixed[f] NR,Z=90 R,Z=94	Line Groups	Rel.[g] Z=94	Line Groups	Agreement[h]: Energy	Int.	Qual. Evid.
$L_2-M_3M_5$	13807-13859	5							0.022		0.015		0.013				
$L_3-M_5N_6$*	13803-13811	3		33b	13807	6	0.146	0.02	0.141	0.176	0.141	0.169	0.057	[0.146][i]	E	R ASS.	S
$L_3-M_5N_7$	13811-13827	3											0.055				
$L_3-M_4O_3$	13868	3							0.010		0.010		0.014				
$L_1-M_3M_3$	13861-13886	9							0.001		0.001		0.002				
18429 M_3	13861	9							~0.001⁺		~0.001⁺		[0]				
$L_3-M_5O_1$	13912	2							0.001		0.001		<0.005				
$L_3-M_4O_4$	13971	5							0.004		0.004		0.004				
$L_3-M_5O_2$	13982	5		34	13951	20	0.043	0.02	0.012	0.048	0.012	0.048	0.005	0.039	P	ALL	W
$L_3-M_4O_5$*	13981	2							0.032		0.032		0.030				
$L_3-M_5O_3$*	14063	3		35	14049	20	0.015	0.01	0.025		0.025		0.020		G	ALL	VW
$L_3-M_5O_4$*	14166	2		36	14159	6	0.102	0.02	0.043	0.098	0.043	0.098	0.039	0.087	G	ALL	M
$L_3-M_5O_5$*	14176	2							0.055		0.055		0.048				
$L_2-M_4M_4$ $^1S_0$*	14200	2	12%	37	14232	10	0.120	0.02	0.146		0.096		0.081		E	NONE M,B	S
$^3P_2$*	14231	2	88%														
$L_2-M_4M_5$*	14411-14431	2							0.655		0.430		0.301				
18429 M_4	14459	8		38a	14420	6	0.347	0.03	N⁺	0.679	N⁺	0.451	N⁺	0.307	G	NONE R,B	VS
$L_1-M_3M_4$	14470-14483	7							0.024		0.021		0.006				
$L_2-M_5M_5$	14584-14622	2		38b	14621	30	0.021	0.015	0.031	0.049	0.021	0.037	0.015	0.019	F	R	VW
$L_1-M_3M_5$	14645-14697	5							0.018		0.017		0.004				
18429 M_5	14654	8							N⁺		N⁺		N⁺				
$L_2-M_1N_1$	14720-14735	5							0.001		0.001		N				
$L_3-N_1N_1$	14895	6		39	14895	31	0.029	0.015	N	0.002	N	0.005	N	0.016	G	R	VW
$K_2-M_1N_2$*	14909-14911	5							0.007		0.005		0.016				
$L_1-M_4M_4$	15038-15069	5							0.002		0.002		0.002				
$L_3-N_1N_2$	15079-15091	6							N		N		N				
$L_2-M_2N_1$*	15110-15112	7		40	15112	15	0.053	0.015	0.013	0.017	0.009	0.012	0.026	0.030	E	NONE R,B	M
$L_2-M_1N_3$	15166-15170	5							0.002		0.001		0.002				
$L_3-N_2N_2$	15252	6							N		N		N				
$L_1-M_4M_5$*	15249-15269	5		41	15258	10	0.144	0.02	0.095	0.120	0.083	0.100	0.069	0.115	G	NONE NR,R,B	S
$L_2-M_2N_2$*	15282-15297	7							0.025		0.017		0.046				
$L_3-N_1N_3$*	15328-15350	6		42	15351	20	0.027	0.015	0.004		0.004		0.009		G	NONE R,B	VW
$L_1-M_5M_5$	15422-15460	5							0.028		0.024		0.019				
$L_2-M_1N_4$	15450-15451	3							0.001		0.001		0.003				
$L_2-M_1N_5$	15497-15498	3							0.001		0.001		N				
$L_3-N_2N_3$*	15513-15519	6							0.008		0.008		0.014				
$L_2-M_2N_3$*	15549-15550	7		43	15563	10	0.123	0.02	0.053	0.096	0.034	0.071	0.056	0.103	G	R	S
$L_1-M_1N_1$*	15558-15573	7							0.005		0.003		0.011				
$L_3-N_1N_4$	15614-15621	4							N		N		N				
$L_3-N_1N_5$	15685-15693	4							0.001		0.001		N				
$L_1-M_1N_2$	15747-15749	7							0.007		0.006		0.012				
$L_3-N_3N_3$*	15764-15775	6		44a	15815	15	0.07	0.02	0.013	0.058	0.013	0.047	0.018	0.062	G	NR,R	M
$L_3-N_2N_4$	15787-15807	4							0.001		0.001		N				
$L_2-M_2N_4$*	15830-15833	5							0.029		0.019		0.028				
$L_3-N_2N_5$*	15839-15844	4							0.007		0.007		0.004				
$L_2-M_1N_6$	15858-15860	3							0.002		0.001		N				
$L_2-M_1N_7$	15870-15872	3		44b	15874	15	0.054	0.015		0.056		0.036	N	0.035	E	NR	M
$L_2-M_2N_5$*	15879-15880	5							0.054		0.035		0.035				

TABLE IV. (*Continued*).

	Predicted Energy			Experimental[d]					Theoretical Intensity						Agreement[h]		
Pu Transition (Auger/ Conversion)	Energy (Spread) Larkins[a] (eV)	Unc.[b]	Intm. Coup. %[c]	Line[d]	Energy (eV)	Unc.	Int.	Unc.	Non-Rel.[e] Z=90	Line Groups	Mixed[f] NR,Z=90 R,Z=94	Line Groups	Rel.[g] Z=94	Line Groups	Energy	Int.	Qual. Evid.
L_1-M_2N_1	15948-15950	8							0.005		0.003		0.008				
L_2-M_1O_1	15963	5							N		N		N				
L_1-M_1N_3*	16004-16008	6							0.013		0.012		0.017				
L_2-M_1O_2	16033	6							0.002		0.001		0.004				
L_3-N_1N_6	16022-16027	5							}0.001		}0.001		N				
L_3-N_1N_7	16036-16039	5											N				
				45	16051	20	0.084	0.02		0.055		0.051		0.069	G	R	W
L_3-N_3N_4*	16051-16057	4							0.011		0.011		0.016				
L_2-M_3N_1	16092-16096	7							0.002		0.001		0.002				
L_3-N_3N_5*	16090-16116	4							0.021		0.021		0.022				
L_2-M_1O_3	16114	3							N		N		N				
L_3-N_1O_1	16123-16129	6							N		N		N				
L_1-M_2N_2	16120-16135	9							N		N		N				
L_3-N_1O_2	16196-16197	7							N		N		N				
L_3-N_2N_6	16200-16208	5							0.001		0.001		0.001				
L_3-N_2N_7	16214-16216	5											0.001				
L_2-M_1O_4	16217	6							N		N		N				
L_2-M_1O_5	16227	3							N		N		N				
L_2-M_2N_6	16238-16244	5							}0.010		}0.007		0.002				
L_2-M_2N_7	16252-16253	5											0.002				
L_3-N_1O_3*	16269-16271	5							0.001		0.001		N				
				46	16294	15	0.07	0.03		~0.057		0.044		0.055	G	ALL NR,R,B	W
L_2-M_3N_2*	16274-16275	7							0.035		0.024		0.038				
L_1-M_1N_4*	16288-16289	6							0.010		0.009		0.011				
L_3-N_2O_1	16303-16304	6							N		N		N				
L_3-N_4N_4	16324-16336	2							0.002		0.002		N				
L_1-M_1N_5*	16335-16336	6							0.016		0.014		0.013				
L_2-M_2O_1	16344	7							0.003		0.002		0.007				
L_3-N_2O_2	16369-16375	7							N		N		N				
L_3-N_1O_4	16375	7							N		N		N				
				47a	16385	15	0.113	0.02		0.082		0.077		0.089	G	NONE R,B	M
L_3-N_4N_5*	16378-16386	2							0.031		0.031		0.034				
L_3-N_1O_5	16383	4							N		N		N				
L_1-M_2N_3	16387-16388	8							0.001		0.001		N				
L_2-M_2O_2	16414	7							0.006		0.004		0.011				
L_3-N_5N_5*	16418-16432	2							0.023		0.023		0.024				
L_3-N_2O_3	16446-16447	5							0.002		0.002		N				
L_3-N_3N_6	16458-16466	5		47b	16474	±20	0.026	0.015	}0.003	0.018	}0.003	0.013	N	0.013	G	ALL	VW
L_3-N_3N_7	16467-16478	5											N				
L_2-M_2O_3*	16495	7							0.013		0.008		0.013				
L_2-M_3N_3	16518-16540	7							0.002		0.002		0.002				
L_3-N_2O_4*	16551-16552	7							N		N		N				
L_3-N_2O_5	16559-16560	4							0.001		0.001		N				
L_3-N_3O_1	16561-16563	6							0.001		0.001		N				
L_2-M_2O_4*	16598	6		48	16576	20			0.006		0.004		0.006		G		VW
L_2-M_2O_5*	16608	6							0.012		0.008		0.007				
L_3-N_3O_2	16631-16632	7							0.002		0.002		N				
L_1-M_2N_4	16668-16671	7					0.059	0.02	N	0.041	N	0.033	0.001	0.035		NR	W
L_2-M_4-N_1	16690-16692	4							0.001		N		0.005				
L_1-M_1N_6	16696-16698	6							0.002		0.001		0.001				
L_3-N_3O_3*	16699-16707	5		49	16683	20			0.006		0.006		0.008		G		VW
L_1-M_1N_7	16708-16710	6							0.002		0.002		0.001				
L_1-M_2N_5	16717-16718	7							0.002		0.002		0.004				
L_3-N_4N_6	16731-16748	3							}0.004		}0.004		N				
L_3-N_4N_7	16745-16758	3											N				

TABLE IV. (*Continued*).

Pu Transition (Auger/ Conversion)	Predicted Energy: Energy (Spread) Larkins[a] (eV)	Unc.[b]	Intm. Coup. %[c]	Experimental[d]: Line[d]	Energy (eV)	Unc.	Int.	Unc.	Theoretical Intensity: Non-Rel.[e] Z=90	Line Groups	Mixed[f] NR,Z=90 R,Z=94	Line Groups	Rel.[g] Z=94	Line Groups	Agreement[h]: Energy	Int.	Qual. Evid.
$L_3-N_5N_6$*	16785-16795	3							0.016		0.016		0.007				
$L_3-N_5N_7$*	16791-16813	3											0.007				
$L_1-M_1O_1$	16801	7		50a	16807	15	0.038	0.02	0.001	0.053	0.001	0.043	0.002	0.033	G	ALL R,B	VW
$L_3-N_3O_4$*	16809-16812	7							0.001		0.001		N				
$L_3-N_3O_5$*	16816-16819	4							0.003		0.003		N				
$L_2-M_3N_4$*	16812-16818	5							0.032		0.022		0.017				
$L_3-N_4O_1$	16841-16842	4							N		N		N				
$L_2-M_3N_5$	16858-16865	5							0.004		0.003		0.003				
$L_2-M_4N_2$*	16870-16873	4		50b	16870	6	0.119	0.02	0.022		0.015		0.019				
18429 N_1*	16870	8							[0.089]	[0.119][i]	[0.098]	[0.119][i]	[0.093]	[0.119][i]	E	ASS.	M
$L_1-M_1O_2$	16871	7							0.001		0.001		0.004				
$L_2-M_5N_1$	16884-16887	4							0.003		0.002		N				
$L_3-N_5O_1$	16889-16890	4							N		N		N				
$L_3-N_4O_2$	16910-16911	5							N		N		N				
$L_1-M_3N_1$*	16930-16934	8							0.008		0.007		0.012				
$L_1-M_1O_3$	16952	7		50c	16955	20	0.022	0.015	0.003	0.016	0.002	0.014	0.003	<0.019	G	ALL	VW
$L_3-N_5O_2$	16958-16959	5							0.003		0.003		N				
$L_3-N_4O_3$*	16983-16986	3							0.002		0.002		<0.004				
$L_3-N_5O_3$*	17030-17033	3							0.005		0.005		0.005				
18429 N_2	17049	9		51	17051	12	0.033	0.02	0	0.049	0	0.037	[0.004]	[0.033][i]	F	ALL M,R,B	W
$L_1-M_1O_4$	17055	7							0.002		0.002		0.002				
$L_1-M_1O_5$	17065	6							0.003		0.002		0.002				
$L_2-M_5N_2$*	17069-17071	4							0.032		0.022		0.019				
$L_1-M_2N_6$	17076-17082	7							0.003		0.002		N				
$L_1-M_2N_7$	17090-17091	7											0.001				
$L_3-N_4O_4$	17084-17091	5							0.004		0.004		N				
$L_3-N_4O_5$*	17096-17099	2							0.006		0.006		>0.007				
$L_1-M_3N_2$	17112-17113	8							0.001		0.001		N				
$L_2-M_4N_3$*	17127-17133	4							0.040		0.026		0.020				
$L_3-N_5O_4$*	17136-17139	5		52a	17126	12	0.044	0.02	0.006	0.065	0.006	0.051	0.007	0.045	F	ALL R,M	W
$L_3-N_5O_5$*	17140-17148	2							0.009		0.009		0.009				
$L_3-N_6N_6$	17137-17154	3							0.002		0.002		N				
$L_3-N_6N_7$*	17156-17167	3											N				
$L_3-N_7N_7$	17163-17178	3											N				
$L_1-M_2O_1$	17182	8							0.001		0.001		0.002				
$L_2-M_3N_6$	17221-17228	6							0.006		0.004		N				
$L_2-M_3N_7$	17230-17239	6		52b	17223	20	0.020	0.015		0.006		0.004		N	E	NR	VW
$L_1-M_2O_2$	17252	9							0.000		0.000		N				
$L_3-N_6O_1$	17251-17252	5							N		N		N				
$L_3-N_7O_1$	17263-17264	5															
18429 N_3	17306	9															
$L_3-N_6O_2$	17320-17321	5							N		N		N				
$L_2-M_5N_3$	17320-17327	4							0.005		0.003		0.003				
$L_3-N_3O_1$	17328	6							0.001		0.001		N				
$L_2-M_3O_1$	17328	7							N		N		N				
$L_3-N_7O_2$	17332	5							N		N		N				
$L_1-M_2O_3$	17333	7							N		N		N				
$L_1-M_3N_3$	17356-17378	8							0.001		0.001		0.001				
$L_2-M_3O_2$*	17398	7							0.008		0.005		0.009				
$L_3-N_6O_3$	17393-17396	3							0.001		0.001		N				
$L_3-N_7O_3$	17404-17407	3															

TABLE IV. (*Continued*).

	Predicted Energy			Experimental[d]					Theoretical Intensity						Agreement[h]		
Pu Transition (Auger/ Conversion)	Energy (Spread) Larkins[a] (eV)	Unc.[b]	Intm. Coup. %[c]	Line[d]	Energy (eV)	Unc.	Int.	Unc.	Non-Rel.[e] Z=90	Line Groups	Mixed[f] NR,Z=90 R,Z=94	Line Groups	Rel.[g] Z=94	Line Groups	Energy	Int.	Qual. Evid.
L_2-M_4N_4*	17396-17418	2		53	17442	7	0.146	0.02	0.057	0.214	0.037	0.141	0.033	0.112	G	M	M
L_1-M_2O_4	17436	7							N		N		N				
L_1-M_2O_5	17446	7							N		0.001		0.001				
L_2-M_4N_5*	17456-17463	2							0.140		0.092		0.066				
L_2-M_3O_3	17479	6							0.001		N		N				
L_3-N_6O_4	17497-17500	6							N		N		N				
L_3-N_6O_5*	17505-17509	3		54a	17535	20	0.032	0.02	0.001	0.010	0.001	0.010	N	0.007	G	NONE NR,B	VW
L_3-N_7O_4*	17510-17513	6							0.001		0.001		N				
L_3-N_7O_5	17517-17521	3							0.002		0.002		N				
L_1-M_4N_1	17528-17530	7							0.007		0.006		0.007				
L_2-M_3O_4	17582	7							0.005		N		0.007				
18429 N_4	17583	8															
L_2-M_3O_5	17592	5							0.001		0.001		N				
L_2-M_5N_4*	17604-17610	2		54b	17614	6	0.073	0.02	0.99	0.123	0.066	0.080	0.052	0.067	G	M,R	M
18429 N_5	17631	8															
L_2-M_5N_5	17646-17653	2							0.012		0.008		0.006				
L_1-M_3N_4	17650-17656	7							0.003		0.003		0.001				
L_1-M_3N_5	17696-17703	7							0.003		0.002		N				
L_1-M_4N_2	17708-17711	7							N		N		0.001				
L_1-M_5N_1	17722-17725	7							0.010		0.009		0.008				
L_2-M_4N_6*	17814-17829	3		55	17834	10	0.054	0.02	0.068	0.083	0.044	0.056	0.007	0.034	E	M,R	VW
L_2-M_4N_7*	17831-17837	3											0.014				
L_1-M_5N_2	17904-17905	7							0.005		0.004		0.005				
L_2-M_4O_1	17926	4							N		N		N				
L_1-M_4N_3	17965	6							N		N		N				
L_2-M_4O_2	17996	5							0.005		0.003		0.004				
L_2-M_5N_6*	18012-18020	3							0.014		0.009		0.004				
L_2-M_5N_7	18020-18036	3															
				56	18068	20	0.035	0.02		0.030		0.023		0.020	E**	ALL NR,B	VW
L_1-M_3N_6	18059-18066	7							0.006		0.006		0.008				
L_1-M_3N_7	18068-18077	7															
L_2-M_4O_3	18077	3							0.005		0.005		0.004				
L_2-M_5O_1	18121	4							N		N		N				

[a] All energies are with respect to the Fermi level. Values, except for L-MO are taken from Larkins (Ref. 7) together with the interchanges of L_3-M_5N_2 and L_3-M_4N_3. For L-MO values see text, Sec. VII. To the experimental energies are added the work function of Al (3.5 eV), see text.

[b] Uncertainties in each of the Larkins values are the combined uncertainties of the three binding energies involved in the transition taken from the Porter and Freedman values used by Larkins in footnote a.

[c] For cases where some intermediate coupling components are widely separated (>20 eV), we get an estimate of the relative importance of the different intermediate coupling components from computations by Haynes (see text, Sec. VII).

[d] Refer to Fig. 1. Lines principally Auger are numbered. Lines principally internal conversion are given capital letters. Experimental intensities (with uncertainties) are given relative to Pu L_3-M_4M_5.

[e] Nonrelativistic theoretical transition probabilities for $Z=90$ were obtained from McGuire (Ref. 5) and Scofield (Ref. 25); see text of Sec. VII. L-shell primary vacancy distribution was taken from Table II. The letter N means the intensity is less than 0.001 (L_3-$M_4M_5=1.0$).

[f] See text of Sec. VII for the description of and reasons for "Mixed" calculation. All rates were divided by the Pu L_3-M_4M_5 rate to get relative intensities. $N<0.001$.

[g] Relativistic theoretical line intensities relative to L_3-M_4M_5 were calculated as described in the text of Sec. VII. N means less than 0.007 because not all transitions were treated in Ref. 8. L-shell primary vacancy distribution was taken from Table II.

[h] This column summarizes qualitatively the agreement in energy and intensity between experiment and theory. The theoretical energy is taken as the energy of the most intense component of the experimental line except where there are two or more nearly equal components, in which case an intensity-weighted average is used in the comparison. The quality of the evidence is dependent primarily on the intensity of the experimental line but also to some extent on its shape. The quality designations are *VS*, very strong; *S*, strong; *M*, medium; *W*, weak; *VW*, very weak. For the intensity agreement we have shown by the symbols NR, nonrelativistic; *M*, mixed; *R*, relativistic; ALL, NONE, those theoretical predictions which were within 1 s.d. (standard deviation). The letter *B* is used when appropriate to indicate the best under conditions of ALL or NONE. The designations for energy agreement are *E*, excellent ($<\frac{1}{2}$ s.d.); *G*, good (<1 s.d.); *F*, fair (<2 s.d.); *P*, poor (>2 s.d.). The double asterisks (**) indicate the following: For line 56 the quality of

TABLE IV. (*Continued*).

the energy agreement depends on which theory is used. For NR and M L_2-$M_5N_{6,7}$ are the most intense, which results in *good* agreement, while for R, L_1-$M_3N_{6,7}$ are the most intense, which results in *excellent* energy agreement. The evidence, however, is not strong.

[i] In some cases there are conversion lines and Auger lines so close together as to be unresolved. Usually in these cases there is no experimental or theoretical information on the intensity of the conversion line. In these cases we have, for each theory, subtracted the total of the theoretical predictions for the included Auger lines from the experimental line intensity to obtain an estimate of the intensity of the internal conversion line. In such cases the line group intensity which was made to equal the experimental intensity, is enclosed in square brackets and the indication ASS. (assigned) is given under the heading "Intensity Agreement." A + sign denotes a conversion line intensity assigned on the basis of an $M1$ multipolarity for the 18.429-keV transition.

We have found a few places in each spectrum where there seemed to be no intensity above the continuous background (β and detector). By a combination of sketching in the background between these points and adding appropriate line tails, we have succeeded in approximating the experimental continuum under the peaks. Each peak was then outlined, including its tail, with reasonable widths where lines were incompletely resolved.

Momenta were determined from the intersect of the upward extrapolated linear sides of the upper half of the line peaks. Spectrometer calibration was based on the $114\,939\pm5$ eV K internal conversion line of the $122\,060\pm4$ eV transition in ^{57}Fe. This was consistent with an internal standard in the ^{239}Pu spectrum which was independently measured, the internal conversion lines of the 7860 ± 3 eV transition (Fig. 1 and Table IV). To the energies determined from these momenta was added the work function of the spectrometer material surrounding and equipotential with the source, aluminum ($\sim$3.5 eV), to refer the Auger energies to the Fermi level of the (metal oxide) source for comparison with Larkins's calculated Fermi-level values. The graphs plot count rate against the setting of the spectrometer instrumental current control potentiometer. Since in a magnetic spectrometer the instrumental linewidth is proportional to momentum, line intensity is proportional to the area of a line (measured via planimeter) divided by its momentum. All intensity measurements were normalized to that of the strongest line, $I_{L_3\text{-}M_4M_5}=1.000$. Auger lines were numbered sequentially while clear conversion lines were lettered A, B, C, etc. in Figs. 1–3 and 5. The results of these energy and intensity measurements are recorded in Table IV for Pu and Table V for Fm and will be discussed in Sec. VIII.

The spectra of Am and Cf (Figs. 5 and 3) have much poorer counting statistics on many lines than the Pu and Fm spectra and have strong spectator vacancy satellites as well. Therefore, analysis of these spectra was attempted only for L-MM lines and the intensity comparisons were only qualitative except for L_i-M_4M_5. The results of these analyses are shown in Tables VI and VII and will also be discussed in Sec. VIII. Finally, quantitative experimental values were obtained for the intensity ratios $I_{L_2\text{-}M_4M_5}/I_{L_3\text{-}M_4M_5}$ for Am and Cf and for the ratio $I_{L_1\text{-}M_4M_5}/I_{L_3\text{-}M_4M_5}$ for Am. A summary of these values together with those for Pu and Fm and comparison with theory is given in Table XIII, to be discussed in Sec. VIII.

VII. THEORETICAL ENERGIES AND INTENSITIES

For energy comparison we have used the semiempirical calculations of Larkins[7] which give the Auger energy values for each total angular momentum J of a given j-j transition referred to the Fermi level. For L_i-M_jO_k, which is not in his tables, we used the $(Z+1)$ approximation,

$$E_{\text{Fermi}}=[B_L(Z)-B_M(Z)-B_O(Z+1)]_{\text{Fermi}}\ .$$

The binding energies used by us for L-MO and by Larkins for all high-Z Augers were those of Porter and Freedman.[12] These are semiempirical interpolations of all heavy-element binding energies for all inner shells. The values are Z-wise smoothed averages of heavy-element data based on all available photoelectron and x-ray spectroscopy, together with values obtained from precision electron spectroscopy of internal conversion electrons in the complex nuclear decays in these same experiments. These latter values are thus intrinsically "fully relativistic" and refer to the Fermi level of the presumably oxide form to which these monolayer source films rapidly convert. Comparison was made[12] to several recent precision relativistic binding-energy calculations, some of which include orbital relaxation and all field-theoretic corrections, and all show a generally monotonically increasing significant deviation with Z above the experimental averages in the transuranic region. Also, because of the compensation for experimental error associated with giving weight to the binding-energy values derived from the same electron spectroscopic measurements, we agree with and accept Larkins's use of the Porter and Freedman values.

The uncertainties in Larkins's and the L-MO values, Tables IV–VII, were calculated from the combination of the three orbital binding uncertainties in Porter and Freedman's values. The uncertainties in Larkin's calculations of the interaction of the final-state vacancies were assumed to be negligible.

For the intensities, we wished to compare both the relativistic and the nonrelativistic Auger theories with our results. Unfortunately, McGuire's[5] nonrelativistic calculations go only to atomic number 90. He was so kind as to supply matrix elements for fermium[23] which Haynes inserted in the equation of Asaad[24] to calculate the L-MM transition probabilities for each J-value member of the intermediate coupling multiplet comprising each "j-j—labeled" transition.[7] These are nonrelativistic estimates. Since the total intensity of each j-j transition relative to that of L_i-M_4M_5 was nearly the same for $Z=100$ as McGuire's value for $Z=90$, it is clear that the nonrelativistic relative intensities within an L_i-MM band are essentially constant from $Z=90$ to 100. We further assumed that the relative intensities $I_{L_i\text{-}X_jY_k}/I_{L_i\text{-}M_4M_5}$, where X stands for M,N,O, etc. and Y for N,O, etc. were constant from $Z=90$ to 100. However, this constancy

TABLE V. *L*-Auger (and internal conversion lines) in ^{254}Fm (and in ^{250}Cf and ^{250}Bk). The superscript α designates transitions in Bk and Cf which follow α decays respectively, of Es and Fm. For discussion of the associated line shapes see the text of Sec. VI. Asterisks (*) indicate those transitions which, according to the criteria of Haynes (Ref. 22) are expected to be the most important.

	Predicted Energy		Experimental					Theoretical Intensity			Agreement[f]		
Transition	eV[a]	Unc.[b]	Peak Desig.	Expt. En. eV.	Unc.	Expt.[c] Int.	Unc.	Theor.[d] Int. Non-Rel.	Theor.[e] Int. Rel.	Line Groups Rel.	En. Agree	Int. Agree Rel.	Qual. Evid.
CfL_3-M_1M_1	6280$^\alpha$	13							0.001	0.001		G	F
FmL_3-M_1M_1	6348	19						0.005	0.003	0.003		G	F
CfL_3-M_1M_2	6713-6740$^\alpha$	10							N	N		G	F
FmL_3-M_1M_2	6796-6822	14	0	6916	38	0.028	0.014	0.008	0.001	0.001	P	P	F
CfL_3-M_2M_2	7122$^\alpha$	13							N	N			
FmL_3-M_2M_2	7219	16	1	7296	20	0.044	0.015	0.002	N	N		G	F
											P	P	F
CfL_3-M_1M_3	7919-7969$^\alpha$	9	2	7882	50	0.046	0.015		0.049	0.049	F	E	F
FmL_3-M_1M_3*	$^3P_1$ 8143	14	3a	8133	4	0.140	0.020	0.076	0.221	0.221	E	G	G
	$^3P_2$ 8193	14	3b	8191	8	0.113	0.018	0.049					
CfL_3-M_2M_3*	8353-8366$^\alpha$	9	4	8368	40	0.083	0.019		0.074	0.074	E	G	F
CfL_3-M_1M_4	8559-8573$^\alpha$	10	5	8576	4	0.315	0.026	0.209	0.010 [±5%]	[±5%] 0.345	F	E	G
FmL_3-M_2M_3*	8593-8607	12							0.335				
CfL_3-M_1M_5	8792-8810$^\alpha$	10	6	8805	12	0.053	0.018	0.016	0.019	0.062	E	G	P
FmL_3-M_1M_4*	8804-8818	14							0.043				
CfL_3-M_2M_4	8966-9009$^\alpha$	10							0.004				
FmL_3-M_1M_5*	9061-9079	15	7a	9065	12	0.261	0.039	0.018	0.098	[0.161][g]	E		F
$BkL_1$34.46*	9204$^\alpha$		7b	9205	8				[0.124 ±0.040]		E		
CfL_3-M_2M_5	9214-9223$^\alpha$	10							0.021				
FmL_3-M_2M_4	9227-9271	12						0.022	0.016				
FmL_3-M_2M_5*	9499-9508	14	8a	9490	4	0.190	0.036	0.177	0.096	0.186	G	E	G
CfL_3-M_3M_3	9563-9589$^\alpha$	11	8b	9565	10				0.090		G	E	G
FmL_3-M_3M_3*	$^3P_0$ 9945	16	9	9956	4	0.493	0.035	0.102	0.417	0.417	G	P	G
	$^3P_2$ 9971	16						0.245					
$BkL_2$34.46*	10089$^\alpha$		Aa	10078	13	0.604	0.046		[0.159 ±0.060]	[0.604][g]			
CfL_3-M_3M_4	10206-10220$^\alpha$	9							0.094				
$BkL_1$35.59*	10334$^\alpha$		Ab	10322	4				[0.235 ±0.06]				
CfL_3-M_3M_5	10422-10477$^\alpha$	9							0.116				
FmL_3-M_3M_4*	10610-10624	12	10	10604	4	0.446	0.045	0.331	0.432	0.432	E	E	E
CfL_3-M_4M_4	10808-10839$^\alpha$	13							0.012				
Fm L_3-M_3M_5 $^3P_1$*, $^3F_3$*	10849-10863	14	11	10853	6	0.571	0.033	0.498	0.523 ±5%	0.535	E	F	E
Fm L_3-M_3M_5 $^1D_2$ $^3F_4$	10889-10905	14						0.057					
CfL_3-M_4M_5*	11062-11082$^\alpha$	10	12	11046	9	0.261	0.036		0.220	0.220	F	F	F
$BkL_2$35.59	11219$^\alpha$								<0.016				
FmL_3-M_4M_4*	11231-11264	16	13	11260	13	0.200	0.035	0.049	0.053	0.200	G	E	F
CfL_3-M_1N_1	11277-11293$^\alpha$	13							N				
CfL_3-M_5M_5*	11275-11314$^\alpha$	13							0.147				
CfL_2-M_1M_1	11482$^\alpha$	13							0.001				
CfL_3-M_1N_2	11484-11486$^\alpha$	13							N				
Fm L_3-M_4M_5 $^3P_1$, $^1G_4^*$	11510-11511	14	14	11508	2	1.000	Std.	0.718	1.000	1.001	E	Std.	E
Fm L_3-M_4M_5 $^1D_2$, $^3F_3^*$	11517-11531	14						0.282					

TABLE V. (*Continued*).

Transition	Predicted Energy eV[a]	Predicted Energy Unc.[b]	Experimental Peak Desig.	Experimental Expt. En. eV.	Experimental Unc.	Experimental Expt.[c] Int.	Experimental Unc.	Theoretical Intensity Theor.[d] Int. Non-Rel.	Theoretical Intensity Theor.[e] Int. Rel.	Theoretical Intensity Line Groups Rel.	Agreement[f] En. Agree	Agreement[f] Int. Agree Rel.	Agreement[f] Qual. Evid.
FmL_3-M_1N_1	11651-11668	18							0.001				
CfL_3-M_2N_1	11703-11705[α]	10							N				
$^3F_2$,$^3F_4^*$	11775-11787	21						0.629					
FmL_3-M_5M_5			15	11782	3	0.615	0.055		0.667	0.676	E	G	E
$^3P_0$	11746	21						0.029					
CfL_3-M_1N_3	11810-11814[α]	9							0.008				
FmL_3-M_1N_2	11869-11871	17							N				
CfL_3-M_2N_2	11891-11908[α]	13							N				
CfL_2-M_1M_2*	11914-11941[α]	10	16	11941	14	0.018	0.011		0.052	0.052	F	P	P
FmL_3-M_2N_1	12093-12096	18							N				
CfL_3-M_1N_4	12116-12117[α]	8							0.001				
FmL_2-M_1M_1	12121	19							0.004				
CfL_3-M_1N_5	12177-12178[α]	8							0.002				
CfL_3-M_2N_3	12228-12230[α]	10							0.014				
FmL_3-M_1N_3*	12237-12241	14							0.038				
FmL_3-M_2N_2	12292-12310	16							N				
FmL_1 39.881	12301	8	B	12286	7	0.129	0.022		[0.022]	[0.129][g]			
CfL_2-M_2M_2*	12323[α]	13							0.047				
CfL_1-M_1M_1	12388[α]	14							0.001				
CfL_3-M_2N_4	12532-12535[α]	8							0.001				
FmL_3-M_1N_4	12554-12555	13							0.006				
CfL_3-M_1N_6	12567-12569[α]	8							0.001				
FmL_2-M_1M_2*	12569-12595	13	17	12562	10	0.170	0.022		0.195	0.209	G	F	G
CfL_3-M_1N_7	12585-12587[α]	8							0.002				
CfL_3-M_2N_5	12594-12594[α]	8							0.004				
FmL_3-M_1N_5	12621-12622	15							0.012				
FmL_3-M_2N_3*	12671-12673	14	18	12658	15	0.063	0.021		0.067	0.079	G	G	F
CfL_3-M_1O_1	12712[α]	11							N				
CfL_3-M_1O_2	12789[α]	14							N				
CfL_1-M_1M_2	12816-12843[α]	11							0.002				
CfL_3-M_1O_3	12891[α]	11							0.002				
CfL_3-M_3N_1	12930-12934[α]	9							0.012				
CfL_3-M_2N_6	12982-12988[α]	8							0.001				
FmL_3-M_2N_4	12986-12989	15							0.003				
FmL_2-M_2M_2*	12992	16	19	12966	5	0.198	0.028		0.213	0.235	F	F	G
CfL_3-M_2N_7	13001-13003[α]	8							0.002				
CfL_3-M_1O_4	13004[α]	11							N				
CfL_3-M_1O_5	13019[α]	11							N				
FmL_3-M_1N_6	13027-13030	14							0.006				
FmL_3-M_1N_7	13046-13049	14							0.010				
FmL_1-M_1M_1	13050	14	20	13046	10	0.048	0.020		0.004	0.035	E	G	P
FmL_3-M_2N_5*	13054-13055	18							0.015				
CfL_3-M_2O_1	13128[α]	11							N				
CfL_3-M_3N_2	13129-13130[α]	12							0.019				
CfL_2-M_1M_3	13120-13170[α]	10							0.004				
FmL_3-M_1O_1	13189	16							N				
CfL_3-M_2O_2	13205[α]	14							N				
CfL_1-M_2M_2	13225[α]	14							N				
FmL_2-39.881			C	13230	1	0.528	0.049		0.502	[0.528][g]			

TABLE V. (*Continued*).

Transition	Predicted Energy eV[a]	Predicted Energy Unc.[b]	Experimental Peak Desig.	Experimental Expt. En. eV	Experimental Unc.	Experimental Expt.[c] Int.	Experimental Unc.	Theoretical Intensity Theor.[d] Int. Non-Rel.	Theoretical Intensity Theor.[e] Int. Rel.	Theoretical Intensity Line Groups Rel.	Agreement[f] En. Agree	Agreement[f] Int. Agree Rel.	Agreement[f] Qual. Evid.
$FmL_3-M_1O_2$	13271	20							N				
$CfL_3-M_2O_3$	13307[α]	11							0.003				
$FmL_3-M_1O_3$	13388	15							0.009				
$CfL_3-M_2O_4$	13420[α]	11							N				
$CfL_3-M_2O_5$	13435[α]	11							0.001				
$CfL_3-M_3N_3$*	13441-13465[α]	9	21	13450	10	0.125	0.021		0.040	0.132	G	E	F
$FmL_3-M_2N_6$	13459-13465	13							0.004				
$FmL_3-M_3N_1$*	13452-13467	17							0.060				
$FmL_3-M_2N_7$	13479-13481	13							0.010				
$FmL_1-M_1M_2$	13498-13524	14							0.008				
$FmL_3-M_1O_4$	13506	15							0.001				
$FmL_3-M_1O_5$	13523	15	22	13536	10	0.089	0.020		0.002	0.094	F	E	F
$CfL_2-M_2M_3$*	13554-13567[α]	10							0.089				
$CfL_3-M_4N_1$	13562-13563[α]	10							0.002				
$FmL_3-M_2O_1$	13621	15							N				
$FmL_3-M_3N_2$*	13674	16	23	13654	10	0.133	0.021		0.089	0.089	F	P	F
$FmL_3-M_2O_2$	13703	19							N				
$CfL_3-M_4N_2$	13759-13763[α]	13							0.001				
$CfL_3-M_3N_4$*	13758-13765[α]	7							0.023				
$CfL_2-M_1M_4$	13760-13774[α]	10							0.009				
$CfL_3-M_5N_1$	13798-13800[α]	10	24	13792	15	0.106	0.021		0.004	0.081	G	F	G
$FmL_3-M_2O_3$	13820	13							0.015				
$CfL_3-M_3N_5$*	13817-13825[α]	7							0.031				
$FmL_1-M_2M_2$	13921	16							N				
$FmL_3-M_2O_4$	13938	14							0.001				
$FmL_3-M_2O_5$	13955	14							0.003				
$FmL_2-M_1M_3$	13966-14016	13							0.012				
$CfL_3-M_5N_2$	13997-13998[α]	13							0.004				
$CfL_2-M_1M_5$	13993-14011[α]	8							0.017				
$FmL_3-M_3N_3$*	14025-14050	14	25a	14032	2				0.182		E		E
$CfL_1-M_1M_3$	14022-14072[α]	11							0.002				
$CfL_3-M_4N_3$*	14086-14092[α]	10				0.318	0.042		0.015	0.293		E	E
$FmL_3-M_4N_1$	14115-14117	17							0.010				
$CfL_2-M_2M_4$*	14157-14210[α]	8	25b	14149	10				0.047		G		P
$CfL_3-M_3N_6$	14210-14218[α]	7							0.003				
$CfL_3-M_3N_7$	14224-14234[α]	7							0.003				
$CfL_3-M_5N_3$*	14320-14327[α]	10							0.020				
$FmL_3-M_4N_2$	14323-14327	16							0.005				
$CfL_3-M_3O_1$	14357[α]	10	26a	14352	2				0.004		G		E
$FmL_3-M_3N_4$*	14354-14361	15							0.106				
$FmL_2-M_2M_3$*	14366-14380	12				0.820	0.063		0.406	0.811		E	E
$FmL_3-M_5N_1$	14375-14378	19							0.023				
$CfL_3-M_4N_4$	14376-14400[α]	8	26b	14402	5				0.004		G		F
$CfL_2-M_2M_5$*	14415-14424[α]	10							0.053				

TABLE V. (*Continued*).

Transition	Predicted Energy eV[a]	Predicted Energy Unc.[b]	Experimental Peak Desig.	Experimental Expt. En. eV	Experimental Unc.	Experimental Expt.[c] Int.	Experimental Unc.	Theoretical Intensity Theor.[d] Int. Non-Rel.	Theoretical Intensity Theor.[e] Int. Rel.	Theoretical Intensity Line Groups Rel.	Agreement[f] En. Agree	Agreement[f] Int. Agree Rel.	Agreement[f] Qual. Evid.
FmL_3-M_3N_5*	14419-14427	18							0.138				
CfL_3-M_3O_2	14434[α]	13							0.005				
CfL_3-M_4N_5*	14450-14457[α]	8							0.036				
CfL_1-M_2M_3	14456-14469[α]	9							N				
CfL_3-M_3O_3	14536[α]	10							0.010				
FmL_2-M_1M_4	14577-14591	13							0.033				
FmL_3-M_5N_2*	14585-14586	18	27	14575	2	0.148	0.021		0.021	0.109	F	P	G
CfL_3-M_5N_4*	14627-14633[α]	8							0.045				
CfL_3-M_3O_4	14649[α]	10							0.004				
CfL_3-M_3O_5	14664[α]	10							0.006				
CfL_1-M_1M_4	14662-14676[α]	10							0.001				
CfL_3-M_5N_5	14671-14700[α]	8	28	14686	10	0.124	0.020		0.056	0.136	E	G	G
FmL_3-M_4N_3*	14691-14698	14							0.069				
CfL_2-M_3M_3	14764-14790[α]	11							0.002				
FmL_3-M_3N_6	14828-14836	13							0.012				
FmL_2-M_1M_5	14834-14852	15	29	14846	15	0.036	0.020		0.009	0.042	E	E	P
CfL_3-M_4N_6	14836-14852[α]	8							0.001				
FmL_3-M_3N_7	14844-14854	13							0.014				
CfL_3-M_4N_7	14859-14865	8							0.004				
CfL_1-M_1M_5	14895-14912	10							0.002				
FmL_1-M_1M_3	14895-14945	14							0.010				
FmL_3-M_5N_3*	14950-14957	16							0.094				
CfL_3-M_4O_1	14989[α]	11	30a	14983	5				N		F	F	
FmL_3-M_3O_1	14992	15							0.016				
FmL_3-M_4N_4	14992-15017	15							0.021				
Fm { $^1P_1$	15000							0.185					
Fm { L_2-M_2M_4*		15				0.715	0.057		0.212	[0.715][g]			
Fm { $^3D_2$	15044							0.003					
BkL_3 34.46	15030[α]	12							[0.148]				
CfL_3-M_4O_2	15066[α]	14	30b	15062	3				N		G		F
FmL_3-M_3O_2	15074	19							0.024				
FmL_3-M_4N_5*	15073-15080	18							0.168				
CfL_3-M_5N_6*	15076-15085[α]	8							0.012				
CfL_1-M_2M_4	15069-15112[α]	11							N				
CfL_3-M_5N_7	15090-15107[α]	8							0.008				
CfL_3-M_4O_3*	15168[α]	11							0.004				
FmL_3-M_3O_3*	15191	13							0.045				
CfL_3-M_5O_1	15226[α]	11							0.001				
FmL_3-M_5N_4*	15267-15271	16	31a	15265	2				0.203		E		
FmL_2-M_2M_5*	15272-15281	14							0.236				
CfL_3-M_4O_4	15281[α]	11							0.001				
CfL_3-M_4O_5	15296[α]	11				1.000	0.070		0.008	0.809		P	E
FmL_1-M_2M_3	15295-15303	13							N				
CfL_3-M_5O_2	15303[α]	14							0.001				

TABLE V. (*Continued*).

Transition	Predicted Energy eV[a]	Predicted Energy Unc.[b]	Experimental Peak Desig.	Experimental Expt. En. eV	Experimental Unc.	Experimental Expt.[c] Int.	Experimental Unc.	Theoretical Intensity Theor.[d] Int. Non-Rel.	Theoretical Intensity Theor.[e] Int. Rel.	Theoretical Intensity Line Groups Rel.	Agreement[f] En. Agree	Agreement[f] Int. Agree Rel.	Agreement[f] Qual. Evid.
FmL$_3$-M$_3$O$_4$	15309	14							0.024				
CfL$_1$-M$_2$M$_5$	15317-15326$^{\alpha}$	11	31b	15320	8				N		E		
FmL$_3$-M$_3$O$_5$	15326	14							0.028				
FmL$_3$-M$_5$N$_5$*	15317-15347	19							0.258				
CfL$_3$-M$_5$O$_3$	15405$^{\alpha}$	11							0.004				
CfL$_2$-M$_3$M$_4$*	15407-15421$^{\alpha}$	9							0.032				
FmL$_3$-M$_4$N$_6$	15476-15492	13							0.006				
FmL$_3$-M$_4$N$_7$*	15499-15507	13	32	15490	5	0.135	0.024		0.021	0.089	G	P	G
FmL$_1$-M$_1$M$_4$	15506-15520	14							0.006				
CfL$_3$-M$_5$O$_4$*	15518$^{\alpha}$	11							0.009				
CfL$_3$-M$_5$O$_5$*	15533$^{\alpha}$	11							0.011				
FmL$_3$-M$_4$O$_1$	15645	15							0.003				
CfL$_2$-M$_3$M$_5$	15623-15678$^{\alpha}$	9							0.005				
CfL$_1$-M$_3$M$_3$	15666-15692$^{\alpha}$	12							N				
FmL$_2$-M$_3$M$_3$	15718-15744	16							0.004				
FmL$_3$-M$_4$O$_2$	15724	19							0.001				
FmL$_3$-M$_5$N$_6$*	15740-15748	15	33	15733	3	0.220	0.021		0.062	0.143	F	P	G
FmL$_3$-M$_5$N$_7$*	15754-15772	15							0.060				
FmL$_1$-M$_1$M$_5$	15763-15781	16							0.008				
FmL$_3$-M$_4$O$_3$	15841	13	34	15824	10	0.019	0.009		0.016	0.016	E	E	P
FmL$_3$-M$_5$O$_1$	15906	16							0.006				
FmL$_1$-M$_2$M$_4$	15929-15973	13							0.001				
FmL$_3$-M$_4$O$_4$	15962	14	35	15964	3	0.071	0.019		0.005	0.045	E	F	G
FmL$_3$-M$_4$O$_5$*	15979	14							0.033				
FmL$_3$-M$_5$O$_2$	15988	20							0.005				
CfL$_2$-M$_4$M$_4$*	16009-16040$^{\alpha}$	13	36a	16036	10				0.030		E		
FmL$_3$-M$_5$O$_3$*	16105	15	36b	16092	10	0.296	0.039		0.022	[0.296][g]	E		G
BkL$_3$-35.59	16164$^{\alpha}$	11							[0.037]				
FmL$_1$-M$_2$M$_5$	16201-16210	15							0.003				
FmL$_3$-M$_5$O$_4$*	16223	16							0.043				
CfL$_3$-N$_1$N$_1$	16237$^{\alpha}$	13	36c	16208	5				N				
FmL$_3$-M$_5$O$_5$*	16240	16							0.053		VP		
CfL$_2$-M$_4$M$_5$*	16263-16283$^{\alpha}$	10							0.108				
CfL$_1$-M$_3$M$_4$	16309-16323$^{\alpha}$	10							N				
FmL$_2$-M$_3$M$_4$*	16383-16397	12	37	16378	5	0.212	0.029		0.133	0.133	E	P	E
CfL$_3$-N$_1$N$_2$	16439-16451$^{\alpha}$	13							N				
CfL$_2$-M$_1$N$_1$	16478-16494$^{\alpha}$	10							N				
CfL$_2$-M$_5$M$_5$	16475-16515$^{\alpha}$	13	38	16498	10	0.018	0.009		0.005	0.005	E	F	P
CfL$_1$-M$_3$M$_5$	16525-16580$^{\alpha}$	10							N				
CfL$_3$-M$_2$N$_2$	16630$^{\alpha}$	21							N				
FmL$_1$-M$_3$M$_3$	16642-16673	16							0.001				
FmL$_2$-M$_3$M$_5$	16636-16678	14							0.017				
CfL$_2$-M$_1$N$_2$	16685-16687$^{\alpha}$	13							0.008				
CfL$_1$-42.720	16710$^{\alpha}$		D	16706	7	0.151	0.027		[0.123]	[0.151][g]			
CfL$_3$-N$_1$N$_3$	16757-16779$^{\alpha}$	10							0.002				

TABLE V. (*Continued*).

Transition	Predicted Energy eV[a]	Predicted Energy Unc.[b]	Experimental Peak Desig.	Experimental Expt. En. eV	Experimental Unc.	Experimental Expt.[c] Int.	Experimental Unc.	Theoretical Intensity Theor.[d] Int. Non-Rel.	Theoretical Intensity Theor.[e] Int. Rel.	Theoretical Intensity Line Groups Rel.	Agreement[f] En. Agree	Agreement[f] Int. Agree Rel.	Agreement[f] Qual. Evid.
CfL_2-M_2N_1	16904-16906[α]	10							0.011				
FmL_3-N_1N_1	16922	29							0				
CfL_1-M_4M_4	16911-16940[α]	14							N				
CfL_3-N_2N_3	16959-16965[α]	10							0.004				
FmL_2-M_4M_4*	17004-17037	16	40	17031	3	0.192	0.028		0.130	0.169	E	G	G
CfL_2-M_1N_3	17011-17015[α]	10							0.001				
CfL_3-N_1N_4	17066-17073[α]	8							N				
CfL_2-M_2N_2	17092-17109[α]	13							0.023				
CfL_3-N_1N_5	17125-17134[α]	8							0.001				
FmL_3-N_1N_2	17133-17146	20							0				
CfL_1-M_4M_5	17165-17185[α]	11							0.002				
$CfL_3N_2N_4$	17255-17277[α]	11							N				
CfL_3-N_3N_3	17279-17290[α]	13							0.004				
FmL_2-M_4M_5*	17284-17304	14	41	17287	2	0.648	0.074		0.465	0.475	E	P	G
FmL_1-M_3M_4	17312-17326	13							0.001				
CfL_2-M_1N_4	17317-17318[α]	8							0.002				
CfL_3-N_2N_5	17321-17326[α]	11							0.001				
FmL_3-N_2N_2	17334	27							0				
CfL_2-M_1N_5	17378-17379[α]	8							N				
CfL_1-M_1N_1	17380-17396[α]	11							N				
CfL_1-M_5M_5	17378-17406[α]								0.001				
FmL_1-44.998	17418		E	17418	1								
CfL_2-M_2N_3	17429-17431[α]								0.023				
FmL_2-M_1N_1	17424-17441								0.001				
FmL_3-N_1N_3	17493-17516								0.010				
CfL_3-N_1N_6	17516-17521[α]								N				
CfL_3-N_1N_7	17535-17539[α]								N				
FmL_2-M_5M_5	17519-17560								0.023				
FmL_1-M_3M_5	17551-17607								0.001				
CfL_1-M_1N_2	17587-17589[α]								N				
CfL_3-N_3N_4	17589-17595[α]								0.004				
CfL_2-42.721	17613												
FmL_2-M_1N_2*	17642-17654								0.034				
CfL_3-N_3N_5	17640-17667[α]								0.004				
CfL_3-N_1O_1	17656-17663[α]								N				
FmL_3-N_2N_3*	17706-17712								0.016				
CfL_3-N_2N_6	17711-17719[α]								N				
CfL_3-N_2N_7	17731-17733[α]								N				
CfL_2-M_2N_4	17733-17736[α]								0.011				
CfL_3-N_1O_2	17739-17740[α]								N				
CfL_2-M_1N_6	17768-17770[α]								N				
CfL_2-M_1N_7	17786-17788[α]								N				
CfL_2-M_2N_5	17795[α]								0.014				
CfL_1-M_2N_1	17806-17808[α]								N				

TABLE V. (*Continued*).

Transition	Predicted Energy eV.[a]	Predicted Energy Unc.[b]	Experimental Peak Desig.	Experimental Expt. En. eV.	Experimental Unc.	Experimental Expt.[c] Int.	Experimental Unc.	Theoretical Intensity Theor.[d] Int. Non-Rel.	Theoretical Intensity Theor.[e] Int. Rel.	Theoretical Intensity Line Groups Rel.	Agreement[f] En. Agree	Agreement[f] Int. Agree Rel.	Agreement[f] Qual. Evid.
$FmL_3-N_1N_4$	17813-17820								0.001				
$CfL_3-N_1O_3$	17835-17836[α]								0.001				
$CfL_3-N_2O_1$	17854-17855[α]		42	17854	8	0.057	0.026		N	0.083	G	F	F
$FmL_2-M_2N_1$*	17866-17869	17							0.055				
$FmL_3-N_1N_5$	17878-17887								0.003				
$CfL_3-N_4N_4$	17883-17895[α]								N				
$CfL_2-M_1O_1$	17913[α]								N				
$CfL_1-M_1N_3$	17913-17917[α]								0.001				
$CfL_3-N_2O_2$	17929-17935[α]								N				
$FmL_1-M_4M_4$	17933-17966								N				
$CfL_3-N_1O_4$	17949[α]								N				
$CfL_3-N_4N_5$	17951-17959[α]								0.008				
$CfL_3-N_1O_5$	17963[α]								N				
$CfL_2-M_1O_2$	17990[α]								0.003				
$CfL_1-M_1N_2$	17994-18011[α]								N				
$CfL_3-N_5N_5$	18003-18018[α]								0.005				
$FmL_2-M_1N_3$	18010-18014								0.004				
$FmL_3-N_2N_4$	18012-18035								0.001				
$CfL_3N_2O_3$	18029[α]								0.001				
$CfL_3-N_3N_6$	18039-18047[α]								N				
$CfL_3-N_3N_7$	18052-18064[α]								N				
$FmL_3-N_3N_3$*	18067-18079	16	43	18064	10	0.060	0.026		0.019	0.133	E	P	F
$FmL_2-M_2N_2$*	18065-18083	18							0.097				
$FmL_3-N_2N_5$	18085-18090								0.004				
$CfL_2-M_1O_3$	18092[α]								N				
$CfL_2-M_3N_1$	18127-18131[α]								0.001				
$CfL_3-N_2O_4$	18142-18143[α]								N				
$CfL_3-N_2O_5$	18156[α]								N				
$CfL_3-N_3O_1$	18181-18183[α]								0.001				
$CfL_2-M_2N_6$	18183-18189[α]								0.001				
$CfL_2-M_2N_7$	18202-18204[α]								0.001				
$CfL_2-M_1O_4$	18205[α]								N				
$FmL_1-M_4M_5$*	18212-18233	15							0.009				
$CfL_1-M_1N_4$	18219-18220[α]								N				
$CfL_2-M_1O_5$	18220[α]								N				
$CfL_3-N_3O_2$	18261[α]								0.001				
$CfL_1-M_1N_5$	18280-18281[α]								N				
$FmL_3-N_1N_6$	18286-18291								0.001				
$FmL_3-N_1N_7$	18306-18310								0.001				
$FmL_2-M_1N_4$	18327-18328								0.008				
$CfL_2-M_2O_1$	18329[α]								0.004				
$CfL_2-N_3N_2$	18330-18332[α]								0.004				
$CfL_1-M_2N_3$	18332-18333[α]								N				
$CfL_3-N_4N_6$	18333-18350[α]								N				
FmL_2-44.988	18347	10	F	18345	2	16.16	1.6		[15.93]	[16.16][g]			
$CfL_3-N_3O_3$	18350-18359[α]								0.002				
$FmL_1-M_1N_1$	18353-18370								N				
$CfL_3-N_4N_7$	18353-18381[α]								0.001				
$FmL_3-N_3N_4$*	18388-18395	16							0.017				
$FmL_2-M_1N_5$	18394-18395								0.001				
$CfL_2-M_2O_2$	18406[α]								0.005				

TABLE V. (*Continued*).

	Predicted Energy		Experimental					Theoretical Intensity			Agreement[f]		
Transition	eV.[a]	Unc.[b]	Peak Desig.	Expt. En. eV.	Unc.	Expt.[c] Int.	Unc.	Theor.[d] Int. Non-Rel.	Theor.[e] Int. Rel.	Line Groups Rel.	En. Agree	Int. Agree Rel.	Qual. Evid.
CfL$_3$-N$_5$N$_6$	18400-18408[a]								0.002				
CfL$_3$-N$_5$N$_7$	18411-18435[a]								0.002				
FmL$_2$-M$_2$N$_3$*	18444-18446	14							0.108				
FmL$_3$-N$_1$O$_1$	18442-18449								N				
FmL$_3$-N$_3$N$_5$*	18445-18473	19							0.022				
FmL$_1$-M$_5$M$_5$	18448-18489								0.003				
CfL$_3$-N$_3$O$_4$	18469-18472[a]								0.001				
CfL$_3$-N$_4$O$_1$	18483-18484[a]								N				
CfL$_3$-N$_3$O$_5$	18482-18485[a]								0.001				
FmL$_3$-N$_2$N$_6$	18491-18499								0.001				
CfL$_2$-M$_2$O$_3$	18508[a]								0.007				
FmL$_3$-N$_2$N$_7$	18512-18514								0.001				
FmL$_3$-N$_1$O$_2$	18529-18530								N				
CfL$_3$-N$_5$O$_1$	18544-18545[a]								N				
CfL$_3$-N$_4$O$_2$	18561-18563[a]								N				
FmL$_1$-M$_1$N$_2$	18571-18573								0.002				
CfL$_2$-M$_2$O$_4$	18621[a]								0.003				
CfL$_3$-N$_5$O$_2$	18623[a]								N				
CfL$_2$-M$_2$O$_5$	18636[a]								0.003				
CfL$_1$-M$_2$N$_4$	18635-18638[a]								N				
FmL$_3$-N$_1$O$_3$	18639-18641								0.002				
FmL$_3$-N$_2$O$_1$	18650-18651								N				
CfL$_2$-M$_3$N$_3$	18642-18666[a]								0.001				
CfL$_3$-N$_4$O$_3$	18656-18660[a]								0.001				
CfL$_1$-M$_1$N$_6$	18670-18672[a]								N				
CfL$_2$-M$_1$N$_7$	18688-18690[a]								N				
FmL$_3$-N$_4$N$_4$	18693-18706								0.001				
CfL$_1$-M$_2$N$_5$	18697[a]								N				
CfL$_3$-N$_5$O$_3$	18716-18720[a]								0.001				
FmL$_3$-N$_2$O$_2$	18729-18736		44a	18728	3				N		P		G
FmL$_3$-N$_1$O$_4$	18759								N				
FmL$_2$-M$_2$N$_4$*	18759-18762	15							0.055				
CfL$_2$-M$_4$N$_1$	18763-18764[a]								0.003				
CfL$_3$-N$_4$O$_4$	18766-18774[a]								N				
FmL$_3$-N$_4$N$_5$*	18767-18776	20				0.160	0.03		0.037	0.203		F	G
FmL$_3$-N$_1$O$_5$	18775								0.001				
CfL$_3$-N$_4$O$_5$	18784-18787[a]								0.002				
CfL$_3$-N$_6$N$_6$	18781-18799[a]		44b	18795	3				N		F		G
FmL$_1$-M$_2$N$_1$	18795-18798								0.001				
FmL$_2$-M$_1$N$_6$	18800-18803								0.001				
CfL$_3$-N$_6$N$_7$	18806-18818[a]								N				
CfL$_1$-M$_1$O$_1$	18815[a]								N				
FmL$_2$-M$_1$N$_7$	18819-18822								N				
CfL$_3$-N$_7$N$_7$	18818-18835[a]								N				
FmL$_2$-M$_2$N$_5$*	18827-18828	18							0.062				
CfL$_3$-N$_5$O$_4$	18831-18834[a]								0.002				
FmL$_3$-N$_5$N$_5$*	18825-18841	24							0.027				
CfL$_3$-N$_5$O$_5$	18840-18850[a]								N				
FmL$_3$-N$_2$O$_3$	18844								0.004				
FmL$_3$-N$_3$N$_6$	18860-18888								0.002				
FmL$_3$-N$_3$N$_7$	18875-18888								0.002				
CfL$_1$-M$_1$O$_2$	18892[a]								N				

[a] All energies are with respect to the Fermi level. Values, except for *L-MO* are taken from Larkins together with the interchange of L_3-M_5N_2 and L_3-M_4N_3. For *L-MO* values see text, Sec. VII. To the experimental energies are added the work function of Al (3.5 eV), see text.

[b] Uncertainties in each of the Larkins values are the combined uncertainties of the three binding energies involved in the transition taken from the Porter and Freedman values used by Larkins in footnote a.

TABLE V. (*Continued*).

[c] Refer to Fig. 2. Lines principally Auger are numbered. Lines principally internal conversion are given capital letters. The experimental intensities of the peaks designated in the Fm and Cf spectra, Fig. 2, are given relative to Fm L_3-M_4M_5.

[d] For cases where some intermediate coupling components are widely separated (>20 eV), we get an estimate of the relative importance of the different intermediate coupling components from computations by Haynes; see text, Sec. VII. These are nonrelativistic estimates.

[e] Relativistic theoretical line intensities relative to L_3-M_4M_5 were calculated as described in the text of Sec. VII. N means less than 0.001. L-shell primary vacancy distribution was taken from Table II.

[f] This column summarizes qualitatively the agreement in energy and intensity between experiment and theory. The theoretical energy is taken as the energy of the most intense component of the line except where there are two or more nearly equal components, in which case an intensity-weighted average is used in the comparison. The quality of the evidence is dependent primarily on the intensity of the experimental line but also to some extent on its shape. The designations are E, excellent; G, good; F, fair; and P, poor. The designations for agreement in energy are E, excellent ($<\frac{1}{2}$ s.d.); G, good (<1 s.d.); F, fair (<2 s.d.); P, poor (>2 s.d.). The agreement in intensity is E, excellent (<1 s.d.); G, good (<2 s.d.); F, fair (<3 s.d.); and P, poor (>3 s.d.).

[g] In some cases there are conversion lines and Auger lines so close together as to be unresolved. Usually in these cases there is no experimental or theoretical information on the intensity of the conversion line. Since the agreement in intensities (relativistic) is generally fairly good, we have used the theoretical intensities of the Auger lines together with the experimental line intensity to obtain an estimate for the intensity of the conversion line. In general, this is the only available experimental evidence on the intensity of the conversion lines.

The tabulated values for the intensities of the L_1, L_2, and L_3 conversion lines of the 34.46- and 35.39-keV transitions in Bk are grossly in error (overestimated) owing to the generally large decay corrections applied to almost all the experimental data based on the $39.3h$ controlling decay of the ^{254m}Es parent. The ^{250}Bk transitions are fed instead by $276d$ ^{254}Es α decay, so their contributions to the intensities of the line complexes are overcorrected. Applying proper decay corrections to these listed Bk components yields much smaller intensity values, but with such relatively large associated errors as to be of little use.

probably does not hold for the Coster-Kronig[25] transitions.

One begins with the initial L_1:L_2:L_3 vacancy distribution (Table II). For Pu we first computed the nonrelativistic intensities relative to L_3-M_4M_5 using McGuire's Auger and Coster-Kronig values for $Z=90$, i.e., ignoring possible CK variation with Z, together with Scofield's[26] relativistic radiation transition probabilities extrapolated to $Z=94$ [by least-squares fit (correlation greater than 0.999) to the fourth root of the transition probabilities from $Z=50$ to 92]. Radiative transition probabilities are needed, together with CK and Auger probabilities, to calculate the CK-generated shifts from the initial L_i vacancy distribution to the distribution needed to calculate the relative Auger emission rates between L_i-XY bands.

In order to allow for possible changes in Coster-Kronig transition probabilities between $Z=90$ and 94, we have also formed a mixed system consisting of McGuire's values for the Auger lines for $Z=90$ and the relativistic Coster-Kronig values of Chen *et al.*[8] for $Z=94$. Finally, we have made a comparison with the complete Auger relativistic calculations of Chen *et al.*[8] interpolated for $Z=94$, using the relativistic radiation calculations of Scofield extrapolated by least squares to $Z=94$.

For fermium the complete set of transition probabilities for $Z=100$ of Chen *et al.*[9] were combined with the least-squares extrapolation of Scofield's radiation probabilities to $Z=100$. No nonrelativistic comparison was attempted because the closest complete Auger calculations were for $Z=90$ (except that the L_i-MM intermediate coupling intensity calculations of Haynes for Fm are nonrelativistic).

These nonrelativistic calculations by Haynes of the relative intensities of the individual J components of an L-MM j-j transition were used for all four spectra in comparing the experimental and theoretical energies of the incompletely resolved L-MM intermediate coupling multiplets (e.g., lines $3a$, $3b$, 9, 11, 14, 15, and 30 in Fig. 2 and 1, 9, 11, 12, 13, and 24 in Fig. 1). With differences of up to 60 eV between the components of different J's, it was important to know which components are dominant.

All of the these theoretical values for energy and intensity are shown in Tables IV (Pu), V (Fm), VI (Am), VII (Cf), and XIII (L_i-M_4M_5 for all four) and will be discussed in Sec. VIII. The tables are fully explained by the accompanying footnotes.

VIII. DETAILED COMPARISON OF THEORY AND EXPERIMENT

A. Energy

We have computed the experimental-theoretical (Larkins) energy difference for each measured line of the four spectra and also the uncertainty in this difference [1 standard deviation (s.d.)]. Table VIII shows the number of lines of each spectrum having differences of various numbers of s.d.'s. Clearly Larkins's values agree with the empirical assignments[16,22] and give correct energies within the experimental errors of the binding energies.

The only clearly resolved intermediate coupling multiplet in an L-Auger transition is that of line L_3-M_1M_3 in Fm (lines $3a$, $3b$ in Fig. 2), although some others show evidence of multiplicity in their rounded peaks, e.g., L_3-M_3M_3 (line 9), whose $^3P_0$ and $^3P_2$ members are split by 26 eV, compared to L_2-M_2M_2 (line 19) with only one member. These Fm structures cannot be attributed to spectator vacancy satellites owing to the low L_1 initial vacancy population [see Fig. 4(c) and Table II]. The energy split in the resolved L_3-M_1M_3 pair closely matches

TABLE VI. *LMM* Auger lines in ^{241}Am. *S* suffix on line label marks spectator vacancy satellite. *J* values are for the final state(s) in intermediate coupling, whose component intensities were calculated by Haynes nonrelativistically for $Z = 100$. Energies are with respect to the Fermi level, corrected (3.5 eV) for the work function of Al (see text). Theoretical [Larkins (Ref. 7)] energy uncertainties are those of Porter and Freedman's binding energies used. Intensities are given qualitatively: *VS* is 1–0.75; *S* is 0.75–0.50; *M* is 0.50–0.25; *W* is 0.25–0.10; *VW* is 0.10–0.01; *VVW* is less than 0.01. *H* (high) and *L* (low) are qualifiers. Intensity predictions are relativistic. Asterisks (*) denote substantial disagreement.

$^{241}_{95}$AM Line	J	Intm. Coup. Comp. (%)	Predictions Larkins (eV)	Exp. Energy (eV)	Expt. Int.	Int. Pred. Rel.	Comments
$L_3-M_1M_1$	0		6,146±5	6,133±16	VVW	VVW	
$L_3-M_1M_2$	1		6,549±6	-	0	VVW	
$L_3-M_2M_2$	0		6,929±10	-	0	VVW	
$L_3-M_1M_3$	2 1	40 60	7,615±6 7,568±6	7,581±15	W	W	Line + Satellite
$L_3-M_2M_3$	2 1	70 30	7,973±8 7,986±8	7,954±8	M	M	Line + Satellite
$L_3-M_1M_4$	2 1	40 60	8,182±6 8,195±6	8,172±24	VW	VW	Line + Satellite
$L_3-M_1M_5$	3 2	60 40	8,401±6 8,384±6	8,342±25	VW	VW	Line + Satellite
$L_3-M_2M_4$	2,1		8,503-8,564	8,606±25	VVW	VVW	Line + Satellite
$L_3-M_2M_5S$				8,694±16	W	-	Sat. of $L_3M_2M_5$
$L_3-M_2M_5$	3,2		8,778-8,789	-	Present	W	Masked by L_1-32.6
$L_3-M_3M_3$	2 0	70 30	9,020±10 8,996±10	-	-	M	Masked by M_1-15.2
$L_3-M_3M_4$	3 2 1	57 23 20	9,613±8 9,630±8 9,618±8	9,612±17	~M	M	On Side of L_2-32.6
$L_3-M_3M_5S$				9,768±10	-	-	Satellite of $L_3-M_3M_5$
$L_3-M_3M_5$	3 1	60 30	9,812±8 9,799±8	9,804±9	M	M	
$L_3-M_4M_4S$				10,167±18	-	-	Satellite of $L_3-M_4M_4$
$L_3-M_4M_4$	2	90	10,221±10	10,228±18	VW	VW	
$L_3-M_4M_5S$				10,370±2	-	-	Satellite of $L_3-M_4M_5$
$L_3-M_4M_5$	4 3	70 20	10,413±8 10,433±8	10,414±2	VS	VS	
$L_2-M_1M_1$	0	100	10,599±5	-	-	VVW	Masked by $L_3M_5M_5$
$L_3-M_5M_5S$				10,577±5	-	-	Satellite of $L_3-M_5M_5$
$L_3-M_5M_5$	4 2	75 20	10,634±10 10,622±10	10,631±10	S	S	
$L_2-M_1M_2$	1	85	10,991±6	10,979±19	VW	VW	
$L_2-M_2M_2$	0	100	11,374±10	11,386±9	W	VW	*
$L_1-M_1M_1$	0	100	11,444±5	11,459±19	VW	VW	
$L_1-M_1M_2$	1 0	80 20	11,847±6 11,872±6	11,843±5	W	W	
$L_2-M_1M_3$	2,1		12,010-12,060	-		VVW	
$L_1-M_2M_2$	0		12,229±10	-	0	VVW	
$L_2-M_2M_3$	2 1	67 33	12,395±8 12,408±8	12,409±5	VW	W	*
$L_2-M_1M_4$	2,1		12,624-12,637	-	-	VW	Masked by $L_3-M_3N_3$
$L_2-M_1M_5$	3,2		12,843-12,826	-	-	VVW	Masked by $L_3-M_3N_4$ SAT, $L_1-M_1M_3$
$L_1-M_1M_3$	2 1	45 55	12,913±6 12,866±6	-	-	W	Masked by $L_3-M_3N_{4,5}$
$L_2-M_2M_4$	1	98	13,003±8	13,004±10	VW	VW	
$L_2-M_2M_5$	3,2		13,220-13,228	-	-	VW	Mixed with $L_3-M_4N_3$
$L_1-M_2M_3$	2	100	13,271±8	-	~0	VVW	
$L_2-M_3M_3$	2,0		13,462-13,438	-	~0	VVW	Interference by $L_3-M_5N_3$, $L_3-M_4N_5$ SAT
$L_1-M_1M_4$	2	90	13,480±6	Present	-	W	Interference by N_2-15.2, $L_3-M_4N_5$ SAT
$L_1-M_1M_5$	3	83	13,699±6	Present	~W	W	Interference by $L_3-M_5N_4$, $L_3-M_5N_5$ SAT
$L_1-M_2M_4$	2,1		13,901-13,859	-	-	VVW	Masked by $L_3-M_4N_7$ SAT
$L_2-M_3M_4$	3	80	14,055±8	-	-	VW	Masked by N_3-15.2
$L_1-M_2M_5$	3	100	14,076±8	-	-	VW	Masked by L_3-32.6
$L_2-M_3M_5$	3 1	60 40	14,254±8 14,241±8	14,262±10	VW	VVW	*
$L_1-M_3M_3$	2	85	14,318±10	-	~0	VVW	
$L_2-M_4M_4$	2	88	14,663±10	14,659±5	M	VW	*
$L_2-M_4M_5$	4	85	14,855±8	14,855±3	M	W	*Includes O_1-15.2276 keV at 14.853 keV, mixed with O_2-15.2276 keV at 14.928 keV.
$L_1-M_3M_4$	3	98	14,911±8	14,924±11	VW	VVW	
$L_2-M_5M_5$	4 2	33 50	15,076±10 15,064±10	15,090±22	VW	VVW	
$L_1-M_3M_5$	3	85	15,110±8	(15,090±22)	(VW)	VVW	
$L_1-M_4M_4$	2 0	40 60	15,519±10 15,488±10	15,502±11	VW	VVW	In partial combination with $L_2-M_2N_1$
$L_1-M_4M_5$	4	99	15,711±8	15,720±2	M	W	*
$L_1-M_5M_5$	4	80	15,932±10	15,957±16	VW	VW	*

TABLE VII. *LMM* Auger lines in ^{250}Cf. See caption for Table VI.

Cf Line	J	Intm. Coup. Comp. (%)	Predictions Larkins (eV)	Expt. Energy (eV)	Expt. Int.	Int. Pred. Rel.	Comments
L_3-M_1M_1	0		6,280±13	-	0	VVW	
L_3-M_1M_2	1		6,713±10	-	0	VVW	
L_3-M_2M_2	0		7,122±12	-	0	VVW	
L_3-M_1M_3	2 1	40 60	7,969±12 7,919±12	7,921±6	W	W	
L_3-M_2M_3	2 1	70 30	8,353±11 8,366±11	8,353±8	M	M	
L_3-M_1M_4	2,1		8,559-8,576	-	D	VW	Poor statistics
L_3-M_1M_5	3 2	60 40	8,810±10 8,792±10	8,785±17	VW	VW	Line + Satellite
L_3-M_2M_4	2,1		8,966-9,009	-	-	VW	On Tail of Conv. Line L_2-34,322
L_3-M_2M_5	3,2		9,214-9,223	-	-	VW	Coincident with L_2-34,322
L_3-M_3M_3	2 0	70 30	9,589±17 9,563±17	9,589±9	M	M	
L_3-M_3M_4S				10,139±19			
L_3-M_3M_4	3 2 1	57 23 20	10,206±12 10,220±12 10,207±12	10,210±4	M	M	
L_3-M_3M_5S				10,385±18			
L_3-M_3M_5	3 1	60 30	10,436±12 10,422±12	10,444±4	HM	LS	
L_3-M_4M_4S				10,783±18			
L_3-M_4M_4	2	90	10,839±13	10,823±18	VW	VW	
L_3-M_4M_5	4 3	70 20	11,062±10 11,082±10	11,065±9	VS	VS	Standard
L_3-M_5M_5	4 2	75 20	11,314±13 11,308±13	11,325±5	S	S	
L_2-M_1M_1	0		11,482±13	-	0	VVW	
L_2-M_1M_2	1	85	11,914±9	11,898±20	W	W	
L_2-M_2M_2	0	100	12,323±11	12,309±20	VW	W	*
L_1-M_1M_1	0	100	12,388±13	-	0	VW	
L_1-M_1M_2	1 0	80 20	12,816±9 12,843±9	12,811±10	VW	VW	
L_2-M_1M_3	2,1		13,170-13,123	-	0	VVW	
L_1-M_2M_2	0	100	13,225±11	13,249±20	VW	VVW	*Doubtful Line Assignment L_3-M_2O_3S ?
L_2-M_2M_3	2 1	67 33	13,554±11 13,567±11	13,543±10	W	W	
L_2-M_1M_4	2,1		13,760-13,777	-	-	VW	Masked by L_3-$M_3N_{4,5}$
?				13,861±10		VW	Unidentified Peak
L_2-M_1M_5	3,2		14,011--13,993	-	-	VVW	On Side of L_1-M_1M_3
L_1-M_1M_3	2 1	45 55	14,072±11 14,022±11	14,051±31	VW	W	* A Real Difference
L_2-M_2M_4	1	98	14,157±9	14,155±20	HVW	LW	On Tail of L_3-34,325
L_2-M_2M_5	3,2		14,415-14,427	-	-	W	Under L_3-34,325
L_1-M_2M_3	2	100	14,456±11	-	-	VW	Under L_3-34,325
L_1-M_1M_4	2,1		14,662-14,776	-	-	VW	Coincident with L_3-M_5N_4
L_1-M_1M_5	3	83	14,913±10	14,918±5	VW	VW	
L_1-M_2M_4	1	83	15,069±9	-	-	VVW	Masked by L_3-$M_5N_{6,7}$
L_1-M_2M_5	3	100	15,317±9	-	-	VW	Masked by L_3-M_4O_5 and L_2-M_3M_4
L_2-M_3M_4	3	80	15,407±11	15,389±22	VW	VW	
L_2-M_3M_5	3 1	60 40	15,637±11 15,623±11	15,619±32	VW	VW	
L_1-M_3-M_3	2	95	15,692±17	-	-	VW	On Tail of L_1-41,740
L_2-M_4M_4	2	88	16,040±13	16,037±22	VW	VW	
L_2-M_4M_5	4 3	85 10	16,263±10 16,283	16,258±6	M	M	
L_1-M_3M_4	3	99	16,309±11	16,281±6			
L_2-M_5M_5	4 2	35 55	16,515±13 16,504±13	16,539±22	VW	VW	
L_1-M_3M_5	3	86	16,539			VVW	
L_1-M_4M_4	2,0		16,942-16,911	-	-	VVW	Masked by L_2-M_2N_1
L_1-M_4M_5	4	99	17,165±10	17,172±23	W	LW	
L_1-M_5M_5	4	80	17,417±13	17,410±23	VW	VW	

Larkins's predictions (Table V). The relative intensity ratio of its components, $I(^3P_1):I(^3P_2)=1.24\pm0.21$, is in fair agreement with the nonrelativistic calculation of Haynes, 1.55 (Sec. VII).

Only seven isolated L-*MO* lines (energies not predicted by Larkins) were observed in Pu and Fm combined. Three of these were within 1 s.d. and three were between 1 and 2 s.d. of the energy predicted by the $\Delta Z=1$ method of Sec. VII, justifying the approximation for E_{LXY} where X and Y differ by at least two shells.

B. Intensity

It is instructive to begin with Pu in order to evaluate nonrelativistic predictions versus relativistic predictions. Table IX shows the results of a statistical comparison based on the results shown in Table IV.

Table IX clearly shows that the agreement with the relativistic theory is superior to either of the others. However, even the relativistic theory falls short of a satisfactory agreement. There is, even for medium or greater quality of line, an excess of three lines with a deviation of greater than 3 s.d. together with a substantial deficit of lines within 1 s.d.

Is the situation similar with Fm? Table X shows the relativistic results for Fm tabulated from the data in Table V. Clearly the agreement is unsatisfactory for Fm, particularly for the stronger lines. For Am and Cf, Tables VI and VII, due to the qualitative nature of the experimental intensity determinations, it is more difficult to draw conclusions. However, six lines in Am and three lines in Cf, each out of 31 total lines, show differences likely to be several standard deviations. Thus none of the four spectra, with the possible exception of Cf, show satisfactory intensity agreement with relativistic theory.

What is the nature of the disagreements? Is theory high or low on the average? Is the agreement perhaps good within a band but not good between bands? Can other generalizations be made which might enable theorists to localize the problem?

First, we looked at the high-low questions. The results, again taken from Tables IV and V for Pu and Fm, are shown in Table XI. With the exception of L_3-*MM* for Pu and the weak lines for Fm, the theoretical predictions are low. However, the L_3-*MM* for Fm is not very low since 12 out of 17 lines are within 1 s.d. Therefore, we can consider the L_3-*MM* band to be well predicted by theory.

In order to examine whether L_2-*MX* and L_3-*XY* bands were perhaps internally consistent, we have normalized each to its strongest line. The procedure does not seem to help, with one important exception. For L_2-$M_jM_{4,5}$ the normalization to L_2-M_4M_5 seems to help for both Pu amd Fm, as shown in Table XII. Hence, it seems that one difficulty with the theory is that the whole L_2-$M_jM_{4,5}$ subband is depressed. The same result can be seen qualitatively for Am (Table VI), where both L_2-M_3M_5 and L_2-M_4M_5 have a substantially lower theoretical than experimental intensity.

Finally, to make the theoretical-experimental difference as sharp as possible, we have accurately measured the intensities of L_3-M_4M_5 and L_2-M_4M_5 for both Am and Cf and also L_1-M_4M_5 for Am. The experimental ratios, together with the same measurements for Pu and Fm from Tables IV and V, are shown in Table XIII.

In calculating the theoretical intensities, we attempted to take into account, in reasonable approximation, the likelihood that the L_3-$M_{4,5}M_{4,5}$ transition probabilities

TABLE VIII. L-Auger energies (experimental vs theoretical). Parentheses indicate Gaussian statistical expectation.

	≤1 s.d.[a]	1–2 s.d.	2–3 s.d.	>3 s.d.
Plutonium *all lines*	44(39)	12(16)	1(3)	1(0)
Medium or greater[b]	27(23)	8(10)	0(2)	0(0)
Americium *all lines*	20(16)	3(6)	0(1)	0
Californium *all lines*	24(17)	0(7)	1(1)	0
Fermium *all lines*	36(34)	15(16)	1(3)	1(0)
Medium or greater[b]	21(19)	5(8)	1(1)	1(0)

[a]Standard deviation.
[b]Quality of evidence, Tables IV–VII.

are reduced when an M_4 or M_5 spectator vacancy exists, owing to the reduced number of electrons available for the transition. We make the assumption that the transition probability is proportional to this number and derive some support for this idea by noting that for Am, it leads to an insignificant change in the calculated relative probabilities for L_3 radiative versus Auger transitions when spectator vacancies exist. The assumption leads to reduction factors for the $L_3M_4M_5$ intensity as follows: Pu, 0.967; Am, 0.940; Cf, 0.954; Fm, 0.976. As other L_3 lines involving M_4 or M_5 vacancies would also be affected, we have calculated the corrections for all these Pu and Fm lines as given in Tables IV and V. All of our calculations used the transition probabilities for Am (Refs. 8 and 26) adjusting only for the different initial vacancy populations, Table II. Note that, although L_2-$M_{4,5}M_{4,5}$ do have spectator vacancy satellites, insufficient energy is available in the preceding L_1-L_2X Coster-Kronig transitions to eject M_4 or M_5 electrons: The spectator vacancies produced are N shell or higher.

Two additional effects should be mentioned. (1) In this part of the Periodic Table L_1-L_3M_3 Coster-Kronig transitions are also possible,[25] giving rise to M_3 spectator vacancies. However, the rate is $\frac{1}{6}$ to $\frac{1}{7}$ of that of the L_1-L_3M_4 and L_1-L_3M_5, respectively, and was neglected. (2) The M_4 and M_5 vacancies are sometimes filled by Auger processes before the L_3 vacancy is filled. In fact, the L_3-level width is about double that of the $M_{4,5}$ widths[15] so that the $M_{4,5}$ levels are filled first about one-third of the time, so that a correction factor of $\frac{2}{3}$ is necessary. This phenomenon was experimentally observed by Frilley *et al.*[27] in the x-ray spectrum of ^{210}Pb→^{210}Bi where the L_1:L_2:L_3 vacancies are in the ratio 90:9:1. The x-ray L_α satellite line (due to $M_{4,5}$ vacancies) should be much stronger than the diagram $L_{\alpha 1}$ line because over 60% of the L_3 vacancies are accompanied by $M_{4,5}$ spectators. In fact, however, the lines are of about equal intensity because some of the $M_{4,5}$ spectator vacancies are filled before the x ray is emitted.

The comparison of the $I_{L_2\text{-}M_4M_5}/I_{L_3\text{-}M_4M_5}$ experimental versus theoretical ratios for Pu, Am, Cf, and Fm and the $I_{L_1\text{-}M_4M_5}/I_{L_3\text{-}M_4M_5}$ ratios for Am are shown in Table XIII. The average $I_{L_2M_4M_5}/I_{L_3M_4M_5}$ experimental to theoretical ratio is 1.27±0.07. Since two of the four elements are within 1 s.d. of this figure, and the other two differ by less than 1.5 s.d., we feel the results of the four elements are consistent with each other and the experimental-theoretical difference is substantial and significant. The same may also be true for L_1-M_4M_5, though we have only one case.

TABLE IX. Intensity comparisons (experiment vs theory) for Pu. Parentheses indicate theoretical expectations.

	≤1 s.d.	1–2 s.d.	2–3 s.d.	>3 s.d.
Nonrelativistic				
All lines	31(44)	20(18)	7(3)	7(0)
Medium or greater[a]	12(33)	8(9)	7(2)	7(0)
Mixed				
All lines	29(44)	22(18)	7(3)	7(0)
Medium or greater[a]	11(23)	10(9)	6(2)	7(0)
Relativistic[b]				
All lines	40(42)	18(17)	1(3)	3(0)
Medium or greater[a]	16(22)	13(8)	0(2)	3(0)

[a]Quality of evidence, column 18, Table IV.
[b]Relativistic has three fewer lines because three lines were used to determine conversion intensities of the 18.429 keV transition. The intensity contribution of these conversion lines was negligible in the three corresponding nonrelativistic and mixed-case comparisons.

TABLE X. Intensity comparisons for Fm.

	<1 s.d.	1–2 s.d.	2–3 s.d.	>3 s.d.
All lines	21(30)	14(11)	8(3)	1(0)
Medium or greater	7(16)	11(6)	4(1)	1(0)

TABLE XI. Are theoretical intensity values high or low? Fractional values arise from the resolution of line complexes, in which different assigned fractions of the total intensity may be low, high, or close to the theoretical values.

	Excellent to good[a]			Fair, poor, very poor[a]		
	High	Low	Close	High	Low	Close
Pu L_3-MM	4	3	0	5	1	1
Pu L_2-MX	2	10.4	0	0.6	7	0
Pu L_3-XY	1	9.3	0.7	0.4	6.9	2
Pu L_1-MM	0	1.5	0.3	1	5.1	0
Fm L_3-MM	2	5	0	5	3	2
Fm L_2-MX	2	5.2	0	4	2	0
Fm L_3-XY	1	6.8	0	3	3	0

[a]Quality of evidence, Tables IV and V. The equivalents for the notation used in Table IV are the following: *VS* is excellent, *S* is good, *M* is fair, *W* is poor, *VW* is very poor.

TABLE XII. Number of lines showing agreement of experimental to theoretical intensities[a] on normalization of L_2-$M_jM_{4,5}$ to L_2-M_4M_5.

	Unnormalized *E G F P*	Normalized *E G F P*
Pu	0 0 2 1	1 1 1 0
Fm	0 1 0 2	1 2 0 0

[a]See footnote f, Table V, for notation on agreement in intensity.

TABLE XIII. Quantitative comparison of L_i-M_4M_5.

Element	L_i-M_4M_5 ratio	Experimental	Relativistic	E/T
Pu	2-45/3-45	0.341±0.03	0.301	1.13±0.1
Am	2-45/3-45	0.33±0.05[a]	0.218	1.54±0.2
Cf	2-45/3-45	0.369±0.04	0.300	1.23±0.13
Fm	2-45/3-45	0.637±0.074	0.476	1.34±0.16
			Average	1.27±0.07
Am	1-45/3-45	0.290±0.03	0.179	1.62±0.16

[a]Experimental intensity of the L_2-M_4M_5 for Am includes the intensity of the O_1 line of the 15.2276-keV transition,[2] which we calculate to be 0.104, relative to L_3-M_4M_5. Hence, to get the experimental intensity of L_2-M_4M_5 for Am, the O_1 intensity was subtracted.

TABLE XIV. Internal conversion of the 18.429-keV transition in ^{239}Pu.

Shell	Line[a]	Expt.	Intensity[b] Theor. $M1$[c]	Theor. $E2$[c]
M_1	23*F*	1.00	1.00	1.00
M_2	25	0.32±0.23	0.133	33
M_3	33*b*	0±0.23	0.01	33
N_1	50*b*	0.72±0.23	0.33	0.33
N_2	51	<0.03±0.23	0.04	10

[a]Figure 1.
[b]Relative to M_1 shell.
[c]Reference 28.

IX. SUMMARY OF L-AUGER RESULTS

Overall, our experimental results on L-Auger intensities in transuranic elements do not agree with relativistic theory except within the L_3-MM band. In general, the theoretical results are too low for all other bands relative to L_3-M_4M_5. In particular, the $I_{L_2M_4M_5}/I_{L_3M_4M_5}$ ratio predictions are low by $(27\pm7)\%$. With respect to Auger energies, our experimental results are in satisfactory agreement with Larkins's intermediate coupling splittings and Haynes's nonrelativistic evaluations of relative intermediate coupling component intensities.

X. NEW NUCLEAR INFORMATION

The resolution of the L-Auger regions of the Pu and Fm spectra yielded a small amount of new nuclear data. Table XIV compares the observed relative M- and N-shell internal conversion coefficients for the 18.429-keV transition in the ^{239}Am (e.c.) ^{239}Pu decay to theoretical $M1$ and $E2$ values.[28] Only an upper limit of 3% per ^{239}Am decay was given[1] for the intensity of this transition from the $\frac{7}{2}^+$, 75.702-keV level to the $\frac{5}{2}^+$, 57.273-keV level of the $\frac{1}{2}^+[631]$ ground-state band in ^{239}Pu. The subshell ratios are consistent with $M1$ multipolarity ($\leq 1\%$ $E2$), although the M_1:N_1 ratio is about 1.5 s.d. away from the theoretical ratio. A complete analysis of the 57 internal conversion lines in ^{254}Fm will be given elsewhere.

ACKNOWLEDGMENTS

We thank Dr. M. H. Chen for the special calculations for Cf and Fm, and Professor Asaad and Professor Larkins for their communications. Preliminary reports of this work were given in the following: in Ref. 17, a general presentation; in Bull. Am. Phys. Soc. **23**, 578 (1978), two abstracts on L-MM spectra; and at the X-ray and Atomic Inner Shell Physics—1982 Conference, Eugene, Oregon, 1982 (unpublished), on the complete spectra of Pu and Fm.

---

*Present address: 625 Harrington Street, Holland, MI 49423.

[1] F. T. Porter *et al.*, Phys. Rev. C **5**, 1738 (1972).
[2] F. T. Porter *et al.*, Phys. Rev. C **10**, 803 (1974).
[3] M. S. Freedman *et al.*, Phys. Rev. C **15**, 760 (1977).
[4] F. T. Porter and M. S. Freedman, Phys. Rev. Lett. **27**, 293 (1971).
[5] E. J. McGuire, Sandia Laboratories Research Report No. SC-RR-710075 (1971) (unpublished).
[6] S. N. E. Ibari, W. N. Asaad, and E. J. McGuire, Phys. Rev. A **5**, 1043 (1972).
[7] F. P. Larkins, At. Data Nucl. Data Tables **20**, 311 (1977); **23**, 587(E) (1979).
[8] M. H. Chen, B. Crasemann, and H. Mark, At. Data Nucl. Data Tables **24** 13 (1979).
[9] M. H. Chen, B. Crasemann, and H. Mark (private communication).
[10] M. S. Freedman *et al.*, Nucl. Instrum. Methods **8**, 225 (1960).
[11] F. T. Porter, M. S. Freedman, F. Wagner, Jr., and I. S. Sherman, Nucl. Instrum. Methods **39**, 35 (1966).
[12] F. T. Porter and M. S. Freedman, J. Phys. Chem. Ref. Data **7**, 1267 (1978).
[13] M. S. Freedman, F. T. Porter, and J. B. Mann, Phys. Rev. Lett. **28**, 711 (1972).
[14] M. S. Freedman and F. T. Porter, Phys. Rev. A **6**, 659 (1972).
[15] O. Keski-Rahkonen and M. O. Krause, At. Data Nucl. Data Tables **14**, 139 (1974); M. O. Krause and J. H. Oliver, J. Phys. Chem. Ref. Data **8**, 329 (1979).
[16] S. K. Haynes, M. Velinsky, and L. J. Velinsky, Nucl. Phys. **A90**, 573 (1967).
[17] M. S. Freedman and F. T. Porter, in Proceedings of the International Conference on Inner Shell Ionization Phenomena and Future Applications, Oak Ridge, Tenn., 1972, edited by R. W. Fink *et al.*[U.S. AEC **1**, 680 (1972), Conf. No. 720404].
[18] D. A. Shirley, Phys. Rev. A **9**, 1549 (1974).
[19] (a) M. H. Chen *et al.*, Phys. Rev. A **19**, 2253 (1979); (b) M. O. Krause, J. Phys. Chem. Ref. Data **8**, 307 (1979).
[20] H. Slätis and M. Rockbarger, Ark. Fys. **40**, 49 (1969).
[21] I. Bergstrom and R. D. Hill, Ark. Fys. **8**, 21 (1954).
[22] S. K. Haynes, in Proceedings of the International Conference on Inner Shell Ionization Phenomena and Future Applications, Oak Ridge, Tenn., 1972, edited by R. W. Fink *et al.* [U. S. AEC **1**, 561 (1972), Conf. No. 720404].
[23] E. J. McGuire (private communication).
[24] W. N. Asaad, Nucl. Phys. **44**, 415 (1963); also, private communication for p initial vacancy, pd final vacancies, $J=0$. The equation is $(1/100)[5D(0)+5D(2)-E(1)-9E(3)]^2$.
[25] In Refs. 8 and 9, L_1-L_3M_3 only becomes energetically possible at $Z=92$, and L_1-L_3M_4 and L_1-L_3M_5 and some other transitions vary by $(5-10)\%$ between $Z=90$ and 100.
[26] J. H. Scofield, Phys. Rev. **179**, 9 (1969).
[27] M. Frilley, B. G. Gokhale, and M. Valdares, C. R. Acad. Sci. **332**, 50 (1951); **332**, 157 (1951).
[28] R. S. Hager and E. C. Seltzer, Nucl. Data Tables A **4**, 1 (1968); O. Dragoun, H. C. Pauli, and F. Schmutzler, *ibid.* **6**, 235 (1969).